ESC European Society of Cardiology

Cardiovascular Research (2022) **118**, 3097–3111
https://doi.org/10.1093/cvr/cvab369

# Loss of myeloid cell-specific SIRPα, but not CD47, attenuates inflammation and suppresses atherosclerosis

**Bhupesh Singla [1†], Hui-Ping Lin[1], WonMo Ahn [1], Jiean Xu [1], Qian Ma [1], Moses Sghayyer [2], Kunzhe Dong[3], Mary Cherian-Shaw[4], Jiliang Zhou[3], Yuqing Huo [1,5], Joseph White[6], and Gábor Csányi [1,3]***

[1]Vascular Biology Center, Medical College of Georgia at Augusta University, 1460 Laney Walker Blvd., Augusta, GA 30912, USA; [2]Medical Scholars Program, Medical College of Georgia at Augusta University, 1460 Laney Walker Blvd., Augusta, GA 30912, USA; [3]Department of Pharmacology and Toxicology, Medical College of Georgia at Augusta University, 1460 Laney Walker Blvd., Augusta, GA 30912, USA; [4]Department of Physiology, Medical College of Georgia at Augusta University, 1460 Laney Walker Blvd., Augusta, GA 30912, USA; [5]Department of Cellular Biology and Anatomy, Medical College of Georgia at Augusta University, 1460 Laney Walker Blvd., Augusta, GA 30912, USA; and [6]Department of Pathology, Medical College of Georgia at Augusta University, 1460 Laney Walker Blvd., Augusta, GA 30912, USA

*Received 24 September 2021; editorial decision 1 December 2021; accepted 17 December 2021; online publish-ahead-of-print 23 December 2021*

**Time for primary review: 30 days**

**Aims** Inhibitors of the anti-phagocytic CD47-SIRPα immune checkpoint are currently in clinical development for a variety of haematological and solid tumours. Application of immune checkpoint inhibitors to the cardiovascular field is limited by the lack of preclinical studies using genetic models of CD47 and SIRPα inhibition. In this study, we comprehensively analysed the effects of global and cell-specific SIRPα and CD47 deletion on atherosclerosis development.

**Methods and results** Here, we show that both SIRPα and CD47 expression are increased in human atherosclerotic arteries and primarily co-localize to $CD68^{+}$ areas in the plaque region. Hypercholesterolaemic mice homozygous for a *Sirpa* mutant lacking the signalling cytoplasmic region ($Sirpa^{mut/mut}$) and myeloid cell-specific *Sirpa*-knockout mice are protected from atherosclerosis. Further, global $Cd47^{-/-}$ mice are protected from atherosclerosis but myeloid cell-specific deletion of *Cd47* increased atherosclerosis development. Using a combination of techniques, we show that loss of SIRPα signalling in macrophages stimulates efferocytosis, reduces cholesterol accumulation, promotes lipid efflux, and attenuates oxidized LDL-induced inflammation *in vitro* and induces M2 macrophage phenotype and inhibits necrotic core formation in the arterial wall *in vivo*. Conversely, loss of myeloid cell CD47 inhibited efferocytosis, impaired cholesterol efflux, augmented cellular inflammation, stimulated M1 polarization, and failed to decrease necrotic core area in atherosclerotic vessels. Finally, comprehensive blood cell analysis demonstrated lower haemoglobin and erythrocyte levels in $Cd47^{-/-}$ mice compared with wild-type and $Sirpa^{mut/mut}$ mice.

**Conclusion** Taken together, these findings identify SIRPα as a potential target in atherosclerosis and suggest the importance of cell-specific CD47 inhibition as a future therapeutic strategy.

*Corresponding author. Tel: +1 706 721 1437; fax: +1 706 721 9799, E-mail: gcsanyi@augusta.edu
[†]Present address: Department of Pharmaceutical Sciences, The University of Tennessee Health Science Center, 881 Madison Ave, Memphis, TN 38163, USA.

## Graphical Abstract

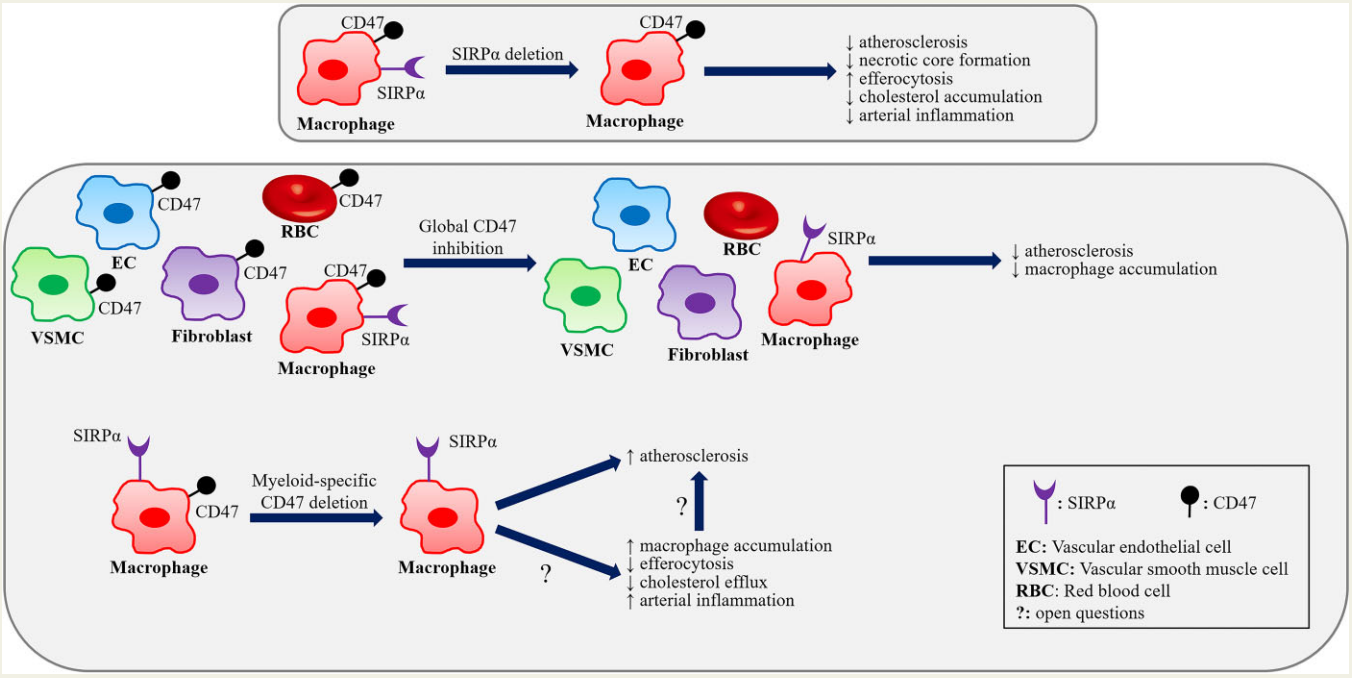


**Keywords** Atherosclerosis • Inflammation • SIRPα • CD47 • Efferocytosis

# 1. Introduction

Immune checkpoint interactions are intercellular regulatory pathways that help maintain tissue homeostasis, in particular by preventing activation of autoimmune-related adverse events.[1] Malignant cells are known to regulate these immune checkpoints to inhibit immune cell activation and prevent their clearance by immune surveillance. Inhibitory signal regulatory protein α (SIRPα) expressed on myeloid cells is an important immune checkpoint receptor that binds to the cell surface glycoprotein CD47. CD47 is ubiquitously expressed on viable cells but rapidly down-regulated during apoptosis, thus, allowing engulfment of apoptotic cells by phagocytes and their subsequent programmed cell removal (aka efferocytosis).[2] Cancer cells, on the other hand, overexpress CD47 that upon binding to phagocyte SIRPα induces a '*don't eat me*' signal to negatively regulate their elimination.[2] Recent studies demonstrated that recombinant polypeptides derived from SIRPα acting as decoy receptors and CD47-blocking antibodies (CD47-Ab) are highly effective to decrease tumour size in a variety of preclinical human tumour xenograft models.[3,4] SIRPα and CD47 blocking pharmacotherapies are now under investigation in clinical trials for both solid and haematologic malignancies.[5,6]

In contrast to the major advances in clinical oncology, pharmacological modulation of immune checkpoints as a therapeutic strategy for the treatment of cardiovascular disease (CVD) is still in its infancy. Pharmacotherapies currently used to treat atherosclerotic vascular disease primarily include lipid-lowering and anti-hypertensive drugs, while ignoring arterial inflammation and other causes of cell death in the vessel wall.[7] The chronic non-resolving inflammation and cell death in atherosclerotic arteries directly contribute to the formation and expansion of necrotic core, which renders plaques unstable, more vulnerable to rupture and arterial thrombosis.[8] As a consequence of plaque rupture, compromised oxygen supply to the heart and brain leads to ischaemic coronary artery disease and stroke, respectively, which are the predominant causes of death and morbidity worldwide.[9] Impaired efferocytosis in advanced atherosclerotic arteries contributes to lesion progression and plaque necrosis.[10] Thus, directly targeting apoptotic cell removal in atherosclerotic arteries may provide therapeutic promise, particularly for those patients who have advanced lesions or had major cardiovascular events despite lipid-lowering therapies and anti-hypertensive medications.

Similar to tumour tissue, CD47 levels are up-regulated in atherosclerotic arteries that may explain why efferocytic clearance of apoptotic cells by macrophages is impaired in advanced plaques.[11] Consistent with dysregulation of SIRPα-CD47 checkpoint inhibition, Kojima *et al.*[11] demonstrated that administration of a blocking CD47-Ab ameliorates atherosclerosis in mice and suppresses vascular inflammation in a small cohort of cancer patients.[12] To our knowledge, no genetic studies have targeted SIRPα in mice and only a single study utilized nanoparticles containing a small molecule inhibitor of SH2 domain-containing phosphatase-1 (SHP-1), a signalling molecule downstream of SIRPα, in atherosclerosis.[13] CD47 is ubiquitously expressed and known to have pleiotropic effects on both immune and non-immune cells.[14] For example, CD47 interacts in *cis* with integrins and VEGFR, binds to thrombospondin 1 (TSP1), and regulates phagocyte SIRPα signalling in *trans*.[15] In contrast, SIRPα expression is more restricted to the central nervous system and macrophages, and its functions independent of efferocytosis

remain largely unknown.[16,17] Although CD47-Ab-induced modulation of immune checkpoints seems a promising strategy in experimental atherosclerosis,[11] translation of these results into the clinic is compromised by the lack of genetic models targeting CD47 and SIRPα in atherosclerosis, limited understanding of cell-specific CD47 and SIRPα signalling in the arterial wall, and largely unknown effects of CD47 and SIRPα blockade on cellular function relevant to atherosclerosis but independent of efferocytosis. Moreover, no pharmacological or genetic studies have investigated the relative efficacy and haematological safety profile of CD47 vs. SIRPα inhibition in atherosclerosis.

In this study, we analysed Western diet-induced atherosclerosis in *Sirpa* mutant, global CD47-deficient, and myeloid cell-specific *Cd47*- and *Sirpa*-knockout mice. We observed that both *Sirpa* mutant and CD47-deficient mice are protected from atherosclerosis. Interestingly, myeloid cell *Sirpa* deletion attenuates atherosclerosis, while myeloid cell-specific *Cd47* knockout mice have increased atherosclerotic lesion formation compared with control mice. Efferocytosis assays demonstrated increased internalization rate of apoptotic cells by *Sirpa*-knockout macrophages. On the contrary, *Cd47* knockout macrophages exhibit suppressed efferocytosis. Independent of efferocytosis regulation, loss of SIRPα reduced macrophage cholesterol accumulation, suppressed nuclear NFκβ levels, and attenuated inflammation. CD47 deficiency reduced macrophage cholesterol efflux, stimulated NFκβ nuclear translocation, and increased arterial inflammation. Finally, haematological analysis demonstrated that *Cd47* knockout mice have lower circulating erythrocyte and haemoglobin levels compared with wild-type and *Sirpa* mutant mice. Taken together, these results identify SIRPα as a therapeutic target in atherosclerosis and highlight the need for future studies to investigate the cell-specific role of CD47 in the arterial wall.

# 2. Methods

## 2.1 Human atherosclerotic tissue

The study was approved by the Biological Safety Office, Augusta University (BSP# 1458) and conducted following the guidelines in the Declaration of Helsinki. The written informed consent was obtained on behalf of each case from the next of kin, for use of cadaveric tissue for research purposes. Human atherosclerotic and non-atherosclerotic aortic and coronary artery tissue were collected from cadaveric donors at the Medical College of Georgia, Augusta University. Additional information about the tissue donors, including the cause of death, comorbidities, and medical history is available in our previous publication.[18]

## 2.2 Sirpa expression in human atherosclerotic and control arteries

To examine *Sirpa* mRNA expression in human non-atherosclerotic and atherosclerotic arteries, the publicly available gene expression data of human atherosclerosis cohorts were downloaded from Gene Expression Omnibus (GSE43292).[19] Gene expression profiling in used cohorts was generated using the Affymetrix Human 5 Gene 1.0 ST Array.

## 2.3 Animals

All animal experimental procedures were performed after getting approval from the IACUC of Augusta University and conducted following the NIH Guide for the Care and Use of Laboratory Animals. Eight- to ten-weeks-old wild-type C57BL/6J (stock # 000664), $Apoe^{-/-}$ (stock # 002052), $Cd47^{-/-}$ (stock # 003173), and LysM Cre (stock # 004781) mice were procured from the Jackson Laboratory (Bar Harbor, USA). $Sirpa^{mut/mut}$ mice were kindly provided by Dr Jeffrey S. Isenberg (University of Pittsburgh, USA). *Sirpa*-floxed ($Sirpa^{f/f}$) mice were provided by Dr Hisashi Umemori, Harvard Medical School, USA. *Cd47*-floxed ($Cd47^{f/f}$) mice were cryorecovered ($Cd47^{tm1a(KOMP)Mbp}$) from frozen germplasm. Myeloid cell-specific *Sirpa*-knockout ($Sirpa^{f/f}$ LysM $Cre^{+/-}$) and *Cd47* knockout ($Cd47^{f/f}$ LysM $Cre^{+/-}$) mice were generated by breeding $Sirpa^{f/f}$ or $Cd47^{f/f}$ mice with LysM Cre transgenic mice. Double knockout $Apoe^{-/-}/Cd47^{-/-}$ mice were generated by crossing $Apoe^{-/-}$ mice with $Cd47^{-/-}$ mice.

To induce liver-specific low-density lipoprotein receptor (LDLR) degradation and hypercholesterolaemia, mice were injected with a recombinant AAV8-PCSK9 [pAAV-PCSK9-hD374Y (human gain-of-function mutant), Vigene Biosciences, Rockville, $1 \times 10^{11}$ VG, *i.p.*] once and fed a Western diet (Envigo, Indianapolis, IN, TD.88137) for indicated time. Mice were anesthetized by isoflurane inhalation (2–3%) and blood was collected in a heparinized syringe via cardiac puncture for further analysis. Mouse aorta and heart were harvested and fixed in 4% paraformaldehyde for 24 h. Heart tissue was embedded in the optimal cutting temperature compound and stored at -80°C until use.

Detailed methods are included in the Supplementary material online.

# 3. Results

## 3.1 SIRPα expression is elevated in human atherosclerotic arteries and SIRPα mutant mice are protected from atherosclerosis

The development of necrotic core is a hallmark of the vulnerable atherosclerotic plaque and atherothrombotic disease.[20] The therapeutic benefit of selectively blocking the '*don't eat me*' receptor SIRPα in myeloid cells in murine atherosclerosis and the role of SIRPα in human atherosclerosis remain unknown. To determine whether *Sirpa* levels are dysregulated in atherosclerotic arteries, we first analysed a publicly available gene expression database (GSE43292) of human carotid artery endarterectomy samples and observed increased *Sirpa* mRNA expression in human atherosclerotic arteries compared with non-atherosclerotic control tissue ($n = 32$; *Figure 1A*). Next, we quantified SIRPα protein expression in human atherosclerotic and non-atherosclerotic tissue using immunoblotting. First, Oil red O (ORO) staining identified the presence of atherosclerotic lesions in the inner curvature (IC) of human aortic arch but not in the descending aorta (DA), consistent with the atherogenic-promoting mechanisms of disturbed blood flow (Supplementary material online, *Figure S1A*). Histopathological examination identified type IV and V lesions in the IC segments of human aortic arch (Supplementary material online, *Figure S1B*). Immunoblotting analysis demonstrated increased SIRPα expression in human atherosclerotic aortic tissue compared with non-atherosclerotic aortic segments (*Figure 1B and D*). Consistently, SIRPα expression was increased in atherosclerotic IC isolated from both male and female $Apoe^{-/-}$ mice (12 weeks Western diet) compared with plaque-free DA segments (*Figure 1C and D* and Supplementary material online, *Figure S1C and D*). These data suggest an association between elevated SIRPα expression and atherosclerotic lesion formation in both sexes.

Next, 8–10 weeks old male wild-type ($Sirpa^{+/+}$) and *Sirpa* mutant ($Sirpa^{mut/mut}$) mice were injected with AAV8-PCSK9 and fed a Western diet for 16 weeks to induce atherosclerosis. $Sirpa^{mut/mut}$ mice express

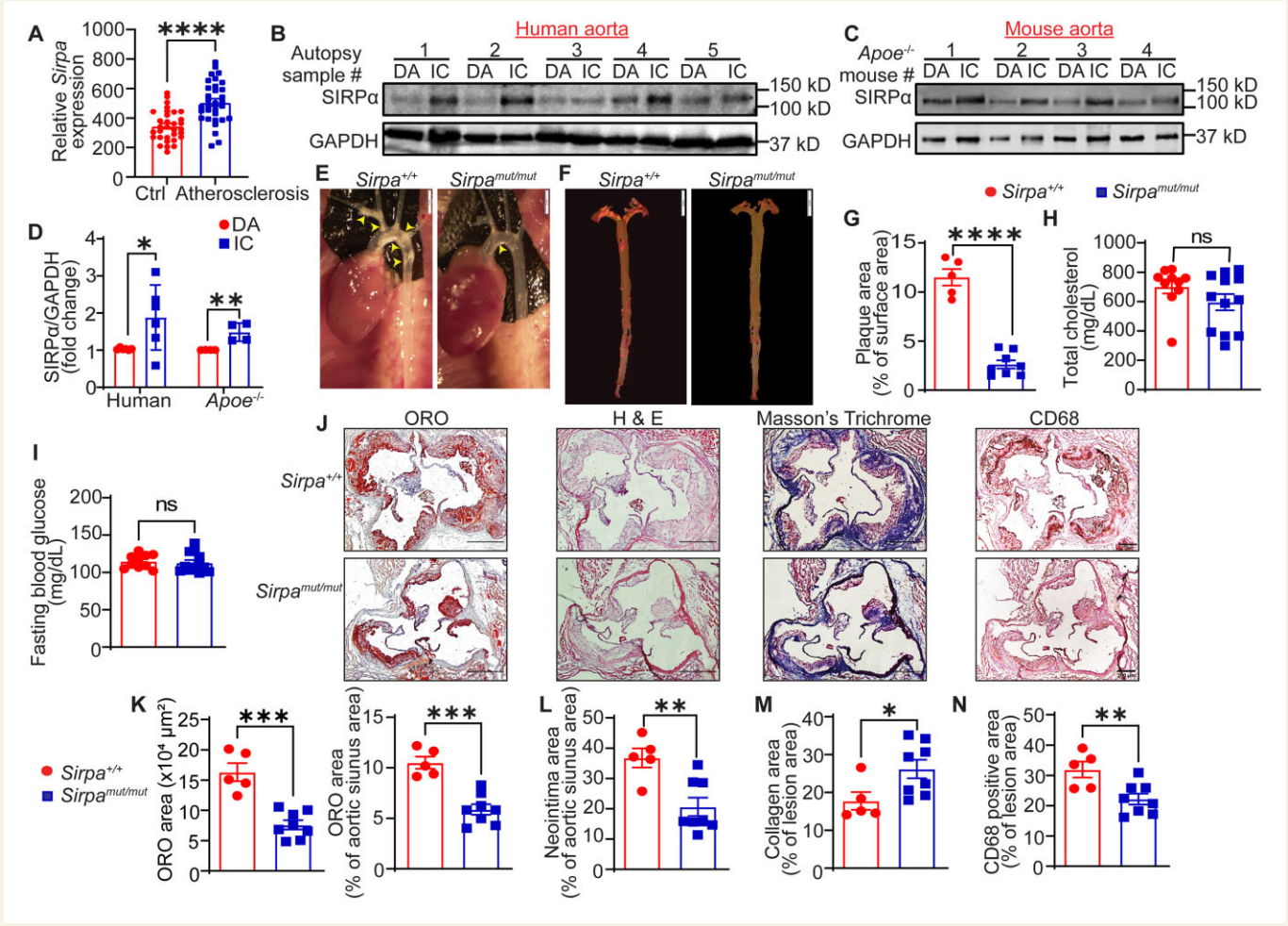


**Figure 1** SIRPα expression is elevated in atherosclerotic arteries and SIRPα mutant mice are protected from atherosclerosis. (*A*) Analysis of available gene expression database (GSE43292) for *Sirpa* mRNA levels in human atherosclerotic arteries and control (Ctrl) tissue ($n = 32$). (*B*) Representative western blot images of SIRPα protein expression in human non-atherosclerotic DA and atherosclerotic IC ($n = 6$). (*C*) Representative western blot images of SIRPα expression in atherosclerotic IC and plaque-free DA segments of male *Apoe*$^{-/-}$ mice fed with a Western diet for 12 weeks ($n = 4$). (*D*) Bar graph represents mean SIRPα protein levels. (*E–N*) Male *Sirpa*$^{+/+}$ and *Sirpa*$^{mut/mut}$ mice were injected with AAV8-PCSK9 *i.p.*, fed a Western diet for 16 weeks, followed by aorta *en face* ORO staining and immunohistochemical analyses of aortic root cross-sections. (*E*) Representative *in situ* images of aortic arch (yellow arrowheads: atherosclerotic lesions), scale bar: 2 mm. (*F*) Representative *en face* ORO staining of aorta, scale bar: 5 mm. (*G*) Quantification of plaque area in aorta ($n = 5–8$). (*H* and *I*) Bar diagrams showing total plasma cholesterol (*H*) and fasting blood glucose levels (*I*). (*J*) Representative images of aortic root cross-sections stained with ORO (lipid accumulation), H & E (neointima area), Masson's Trichrome (collagen content), scale bar: 400 µm and CD68 (macrophage burden), scale bar: 200 µm. (*K–N*) Lipid deposition (*K*), neointima area (*L*), collagen content (*M*), and macrophage accumulation (*N*) in aortic root sections ($n = 5–8$). Statistical analyses were performed using a two-tailed unpaired *t*-test. Data represent mean ± SEM. *$P < 0.05$, **$P < 0.01$, ***$P < 0.001$, and ****$P < 0.0001$.

SIRPα with an intact extracellular domain that can interact with CD47, however, it lacks majority of the cytoplasmic region, which prevents its tyrosine phosphorylation and abrogates its ability to form a complex with SHP-1 or SHP-2 in phagocytes to inhibit efferocytosis.[21] On the other hand, complete SIRPα deletion leads not only to inhibition of intracellular SIRPα signalling in phagocytes but can also modify CD47 signalling in vascular cells, immune cells (*trans*) and may even have autocrine actions (*cis*). For example, deletion of the extracellular SIRPα domain in macrophages may 'free up' CD47 in vascular cells that via binding to TSP1 (soluble ligand for CD47) have SIRPα-independent effects.[15] Animal genotypes were determined and protein expression in aortic and liver tissue lysates was verified using an antibody[22] targeting the cytoplasmic tail of SIRPα protein (Supplementary material online, *Figure S1E and F*). *En face* ORO staining of the aorta demonstrated substantially reduced atherosclerosis in *Sirpa*$^{mut/mut}$ mice [% plaque area: 2.63 ± 0.42 (77.6% decrease)] compared with wild-type controls (11.49 ± 0.84), suggesting a detrimental role for SIRPα in the pathogenesis of atherosclerosis (*Figure 1E–G*). Plasma total cholesterol levels, fasting blood glucose, body composition and weight gain were not different between wild-type and *Sirpa*$^{mut/mut}$ mice (*Figure 1H and I* and Supplementary material online, *Figure S1G and H*). Additionally, ORO staining performed on aortic root cross-sections from *Sirpa*$^{mut/mut}$ mice exhibited significantly reduced atherosclerotic lesion area compared with wild-type tissue (7.61 ± 0.78 × $10^4$ µm$^2$ vs. 16.31 ± 1.49 × $10^4$ µm$^2$; $P = 0.0001$) (*Figure 1J and K*). Furthermore, histological staining indicated attenuated neointima area (43.9%), decreased CD68$^+$ area (30.5%), and increased collagen content

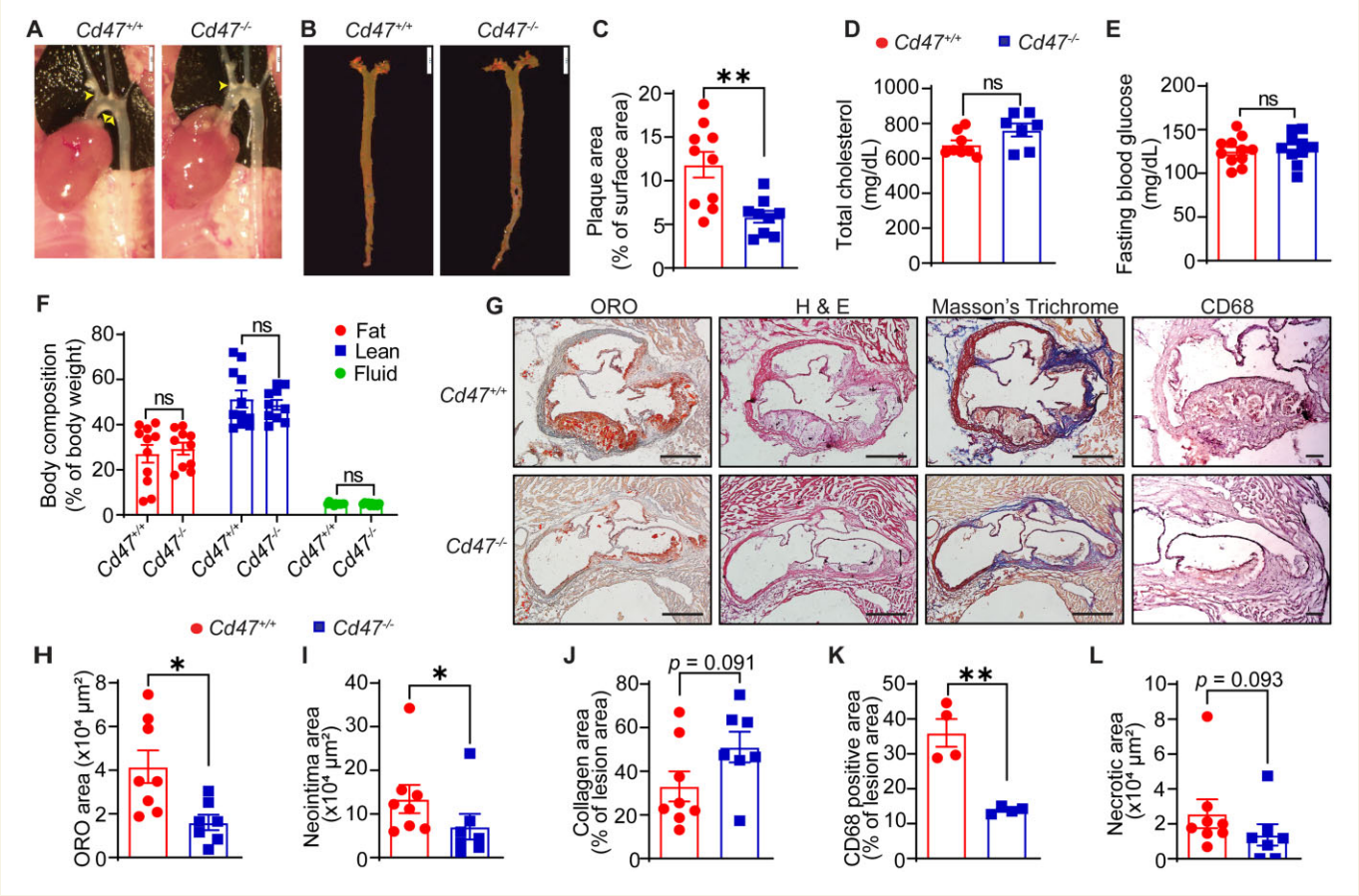


**Figure 2** Global CD47 deficiency suppresses atherosclerosis in hypercholesterolaemic mice. (*A–L*) Male *Cd47*$^{+/+}$ and *Cd47*$^{-/-}$ mice were injected with AAV8-PCSK9 *i.p.*, fed a Western diet for 12 weeks, and analysed for atherosclerosis. (*A*) Representative *in situ* images of aortic arch (yellow arrowheads: atherosclerotic lesions), scale bar: 2 mm. (*B*) Representative *en face* ORO staining of aorta, scale bar: 5 mm. (*C*) Quantification of plaque area in aorta ($n$ = 9–10). (*D–F*) Bar diagrams show total plasma cholesterol (*D*), fasting blood glucose levels (*E*), and body composition (fat, lean, and fluid mass, *F*) ($n$ = 7–11). (*G*) Representative images of staining performed on aortic root cross-sections, scale bar: 400 µm and CD68, scale bar: 100 µm. (*H–L*) Lipid deposition (*H*) ($n$ = 7–8), neointima area (*I*) ($n$ = 7–8), collagen content (*J*) ($n$ = 7–8), macrophage accumulation (*K*) ($n$ =4), and necrotic area (*L*) ($n$ = 7–8) in aortic root sections. Statistical analyses were performed using a two-tailed unpaired *t*-test (*C–E, H, J*, and *K*), two-way ANOVA followed by Sidak's *post hoc* test (*F*), and two-tailed unpaired Mann–Whitney test (*I* and *L*). Data represent mean ± SEM. *$P$ < 0.05 and **$P$ < 0.01.

(47.6%) in *Sirpa*$^{mut/mut}$ mice compared with control animals (*Figure 1J and L–N*). Finally, necrotic area was significantly smaller in *Sirpa*$^{mut/mut}$ mice compared with control animals (Supplementary material online, *Figure S1I*). Collectively, these data demonstrate that SIRPα protein levels are increased in atherosclerotic arteries and SIRPα signalling contributes to atherosclerosis development.

## 3.2 Global CD47 deficiency protects hypercholesterolaemic mice from atherosclerosis

Kojima *et al.*[11] reported up-regulated CD47 levels in atherosclerotic plaques compared with non-atherosclerotic vascular tissue and demonstrated attenuated atherosclerosis in male *Apoe*$^{-/-}$ mice treated with a CD47-Ab. A study using genetic models has reported an atheroprotective effect of CD47 in female mice but did not investigate atherosclerosis in male *Cd47*$^{-/-}$ animals.[23] To investigate the effects of global CD47 deficiency on atherosclerosis development, male wild-type (*Cd47*$^{+/+}$) and *Cd47*$^{-/-}$ mice were injected with AAV8-PCSK9 and fed a Western diet. *En face* atherosclerotic lesion analysis indicated attenuated (50.5%) atherosclerosis in *Cd47*$^{-/-}$ mice (% plaque area: 5.87 ± 0.68) compared with controls (% plaque area: 11.84 ± 1.47; $P$ = 0.0025) (*Figure 2A–C*). There were no significant differences in the metabolic profile between wild-type and *Cd47*$^{-/-}$ mice (*Figure 2D–F*). Further, global CD47 deficiency suppressed plaque area, neointima area, and macrophage accumulation in the aortic root compared with control mice (*Figure 2G–K*). In contrast to *Sirpa*$^{mut/mut}$ mice, no significant differences in the necrotic area were observed between control (2.58 ± 0.83 × $10^4$ µm$^2$) and CD47-deficient animals (1.37 ± 0.61 × $10^4$ µm$^2$) (*Figure 2L*).

Next, to confirm these results with mice on the *Apoe*$^{-/-}$ background, we generated *Apoe*$^{-/-}$/*Cd47*$^{-/-}$ mice. As shown in Supplementary material online, *Figure S2A and B*, atherosclerosis in the aorta of male *Apoe*$^{-/-}$/*Cd47*$^{-/-}$ mice was significantly decreased [% plaque area: 7.90 ± 1.16 (46.7% decrease)] compared with sex-matched *Apoe*$^{-/-}$ controls (14.79 ± 1.09). Plasma total cholesterol, fasting blood glucose, and body composition were not affected by CD47 deficiency in male animals (Supplementary material online, *Figure S2C–E*). Similarly, female *Apoe*$^{-/-}$/*Cd47*$^{-/-}$ mice were protected from atherosclerosis development

[% plaque area: 19.95 ± 2.18 and 30.97 ± 1.98 for *Apoe*$^{-/-}$/*Cd47*$^{-/-}$ and *Apoe*$^{-/-}$ mice, respectively (35.6% decrease)] (Supplementary material online, *Figure S2F and G*). Plasma total cholesterol levels, fasting blood glucose, and body composition were not different (Supplementary material online, *Figure S2H–J*). Taken together, these results indicate that both male and female CD47-deficient mice are protected from atherosclerosis. In addition, our results also suggest that systemic inhibition of SIRPα-mediated signalling may be more effective to attenuate the necrotic core area in murine atherosclerosis models compared to global CD47 inhibition.

## 3.3 Myeloid cell-specific SIRPα deletion suppresses atherosclerotic lesion formation

According to various RNA expression datasets, including the Genotype-Tissue Expression database (gtexportal.org) and BioGPS (biogps.org), and published literature,[17,24] SIRPα is mainly expressed in myeloid cells, hepatocytes, and neuronal cells. To identify the cell type(s) in atherosclerotic arteries expressing SIRPα, immunostaining experiments for SIRPα along with the macrophage marker CD68 and vascular smooth muscle cell (SMC) marker smooth muscle actin (SMA) were performed using human atherosclerotic left anterior descending (LAD) coronary arteries. Histological analysis identified advanced lesions (type Vb, as per American Heart Association classification[25]) with intimal thickening and presence of necrotic core with fine granular calcifications (*Figure 3A*). Immunostaining indicated that SIRPα primarily co-localizes with CD68$^{+}$ areas in the plaque region and minimal co-localization of SIRPα was observed with SMA staining in the medial layer and plaque area (*Figure 3B–D*). To investigate the role of macrophage SIRPα in atherosclerotic lesion formation, myeloid cell-specific *Sirpa*-knockout mice were generated. The genotypes of mice were determined using polymerase chain reaction (PCR) (Supplementary material online, *Figure S3A*) and deletion of SIRPα in myeloid cells was confirmed (Supplementary material online, *Figure S3B*). PCSK9-AAV8-injected *Sirpa*$^{f/f}$ LysM Cre$^{+/-}$ mice and littermate *Sirpa*$^{f/f}$ mice were fed a Western diet for 16 weeks. *En face* ORO staining of the aorta demonstrated significantly suppressed (53%) atherosclerosis in *Sirpa*$^{f/f}$ LysM Cre$^{+/-}$ mice (% plaque area: 4.19 ± 0.50) compared with *Sirpa*$^{f/f}$ controls (% plaque area: 8.91 ± 0.99) (*Figure 3E–G*). As shown in *Figure 3H and I* and Supplementary material online, *Figure S3C and D*, there were no differences in the metabolic profile and blood pressure between myeloid cell-specific *Sirpa* knockout and control mice. Interestingly, we observed increased fat mass and decreased lean mass in *Sirpa*$^{f/f}$ LysM Cre$^{+/-}$ mice (Supplementary material online, *Figure S3E*). Further analyses of aortic root sections demonstrated decreased lesion area (6.78 ± 0.52 × $10^4$ μm$^2$ vs. 12.17 ± 1.05 × $10^4$ μm$^2$; $P = 0.0005$), reduced neointima formation (32.5%), higher collagen content (102.2%), and attenuated CD68$^{+}$ area (39.7%) in *Sirpa*$^{f/f}$ LysM Cre$^{+/-}$ mice in comparison to *Sirpa*$^{f/f}$ controls (*Figure 3J–P*). Furthermore, the necrotic core area was significantly reduced in *Sirpa*$^{f/f}$ LysM Cre$^{+/-}$ mice compared with *Sirpa*$^{f/f}$ mice (Supplementary material online, *Figure S3F*). Consistent with reduced atherosclerosis in male mice, female *Sirpa*$^{f/f}$ LysM Cre$^{+/-}$ had reduced atherosclerotic lesion formation compared with *Sirpa*$^{f/f}$ controls (Supplementary material online, *Figure S4A–G*). These results suggest that deletion of SIRPα selectively in myeloid cells is sufficient to attenuate atherosclerosis development in both male and female mice and decrease necrotic core area in atherosclerotic arteries.

## 3.4 Myeloid cell-specific deletion of CD47 increases atherosclerotic lesion formation

CD47 serves as the *trans*-counter receptor for SIRPα, functions as a signalling receptor for TSP1, and is functionally associated in *cis* with integrins and VEGFR.[15,26] A previous study demonstrated increased CD47 expression in macrophages and foam cell-rich areas of human atherosclerotic arteries.[11] To date, no previous studies have targeted CD47 selectively in myeloid cells in murine models of atherosclerosis. Immunostaining analysis performed on human atherosclerotic LAD showed increased CD47 expression in the necrotic core and CD68$^{+}$ area but not in SMA-positive cells in the medial layer (*Figure 4A and B*). To investigate the role of macrophage CD47 receptor in atherosclerosis, myeloid cell-specific *Cd47* knockout mice were generated (Supplementary material online, *Figure S5A*). Contrary to our expectations, we observed significantly larger (75.5%) atherosclerotic plaque area in the aorta isolated from *Cd47*$^{f/f}$ LysM Cre$^{+/-}$ mice (% plaque area: 10.30 ± 0.98) compared with *Cd47*$^{f/f}$ controls (5.87 ± 0.57) (*Figure 4C–E*). Consistent with these results, aortic root analysis showed larger atherosclerotic lesion area (18.35 ± 0.82 × $10^4$ μm$^2$ vs. 14.40 ± 1.23 × $10^4$ μm$^2$; $P = 0.0062$), augmented neointima formation (19.2%), and increased CD68$^{+}$ area (110.7%) in *Cd47*$^{f/f}$ LysM Cre$^{+/-}$ mice compared with control mice (*Figure 4H–J and L*). No differences in collagen content (*Figure 4H and K*) and necrotic core area (Supplementary material online, *Figure S5D*) were found between the groups. Furthermore, as shown in *Figure 4F and G* and Supplementary material online, *Figure S5B and C*, there were no significant differences in the metabolic profile between myeloid cell-specific *Cd47* knockout mice and control mice. Altogether, these findings suggest that myeloid cell-specific CD47 deletion stimulates atherosclerosis development in hypercholesterolaemic mice.

## 3.5 Macrophage SIRPα deficiency stimulates, but macrophage CD47 deletion inhibits efferocytosis

The interaction of macrophage SIRPα with CD47 inhibits phagocytosis.[17,20] However, the role of macrophage CD47 in regulating efferocytosis is not well characterized. We utilized bone marrow-derived macrophages (BMM) from control and myeloid cell-specific *Sirpa*-knockout mice and quantified internalization of apoptotic cells using confocal microscopy and flow cytometry. Apoptosis of K562 cells after UV exposure was confirmed with Annexin V staining (Supplementary material online, *Figure S6A*). Treatment of wild-type (*Sirpa*$^{f/f}$) macrophages with CD47-Ab increased internalization of apoptotic K562 cells (Deep Red$^{+}$) compared with IgG treatment (*Figure 5A and C*). Efferocytosis of apoptotic cells by SIRPα-deficient BMM was higher in comparison to wild-type controls (*Figure 5A and C*). CD47-Ab treatment did not stimulate efferocytosis in SIRPα-deficient macrophages, consistent with interruption of *trans* CD47-SIRPα signalling prior to antibody treatment (*Figure 5B and C*). Similar results were obtained using flow cytometry (*Figure 5D and E*). In addition, no differences in efferocytic potentials of BMM from *Sirpa*$^{mut/mut}$ and *Sirpa*$^{f/f}$ LysM Cre$^{+/-}$ mice were observed (Supplementary material online, *Figure S6B*). Consistent with increased efferocytosis by SIRPα-deficient macrophages *in vitro* and reduced necrotic core area in the aortic root of *Sirpa*$^{f/f}$ LysM Cre$^{+/-}$ mice compared with *Sirpa*$^{f/f}$ controls (Supplementary material online, *Figure S3F*), *Sirpa*$^{f/f}$ LysM Cre$^{+/-}$ mice had lower number of free apoptotic cells (apoptotic cells not associated with CD68$^{+}$ cells) in the lesion area, indicating increased efferocytosis by SIRPα-deficient macrophages *in vivo* (Supplementary

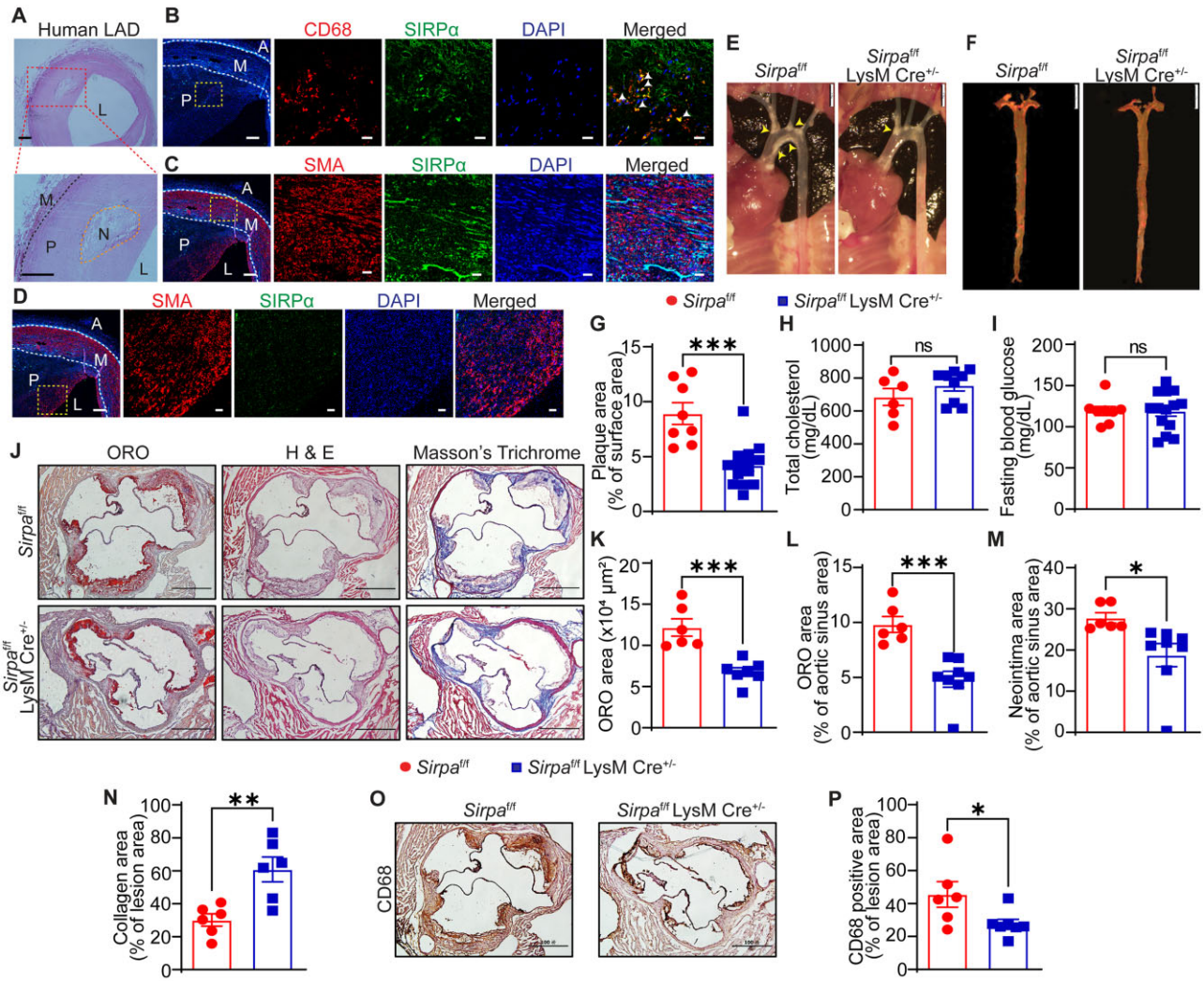


**Figure 3** Myeloid cell-specific SIRPα deficiency reduces atherosclerotic lesion formation. (*A*) Representative images of H & E staining demonstrating the presence of atherosclerotic lesion (P) and necrotic core (N) in human atherosclerotic LAD coronary artery, scale bar: 200 µm. (*B*) Immunostaining was performed on consecutive human LAD cross-sections to investigate CD68 (macrophage marker, red) and SIRPα (green) expression, and sections were counterstained with DAPI (blue), scale bar: 50 and 20 µm. White arrowheads indicate co-localization of CD68 and SIRPα ($n = 4$). (*C* and *D*) Human LAD cross-sections were immunostained for SMA (SMC marker, red) and SIRPα (green) ($n = 4$), scale bar: 50 and 20 µm. (*G–P*) Male *Sirpa*$^{f/f}$ and *Sirpa*$^{f/f}$ LysM Cre$^{+/-}$ mice were injected with AAV8-PCSK9 *i.p.*, fed a Western diet for 16 weeks, and atherosclerosis analysed. (*E*) Representative *in situ* images of aortic arch (yellow arrowheads: atherosclerotic lesions), scale bar: 2 mm. (*F*) Representative *en face* ORO staining of aorta, scale bar: 5 mm. (*G*) Quantification of plaque area in aorta ($n = 8–14$). (*H* and *I*) Bar diagrams showing total plasma cholesterol (*H*) and fasting blood glucose levels (*I*). (*J*) Representative images of staining performed on aortic root cross-sections, scale bar: 400 µm. (*K–N*) Lipid deposition area (*K* and *L*), neointima area (*M*), and collagen content (*N*) in aortic root sections ($n = 6–8$). (*O* and *P*) Macrophage accumulation. Statistical analyses were performed using a two-tailed unpaired *t*-test. Data represent mean ± SEM. *$P < 0.05$, **$P < 0.01$, and ***$P < 0.001$.

material online, *Figure S6C*). Next, efferocytosis experiments were performed using CD47-deficient macrophages to investigate whether disruption of *cis* SIRPα-CD47 interaction in the phagocyte membrane regulates internalization of apoptotic cells. As shown in *Figure 5F*, efferocytosis of apoptotic cells by *Cd47* knockout macrophages was significantly decreased compared with wild-type controls, suggesting that (i) release of SIRPα from macrophage *cis* CD47 interaction promotes the 'don't eat me' signal or (ii) loss of CD47 directly interferes with the phagocytic activity of macrophages. To investigate this further, we compared SHP-1 phosphorylation in wild-type and *Cd47* knockout macrophages and found no differences in the ratio of pSHP-1/total SHP-1 proteins, suggesting no regulation of SIRPα-mediated phagocytic activity in CD47-deficient cells (Supplementary material online, *Figure S6D*). Taken together, these results demonstrate that inhibition of SIRPα signalling in macrophages stimulates clearance of apoptotic cells *in vitro* and *in vivo*. Our results also suggest that non-selective pharmacological

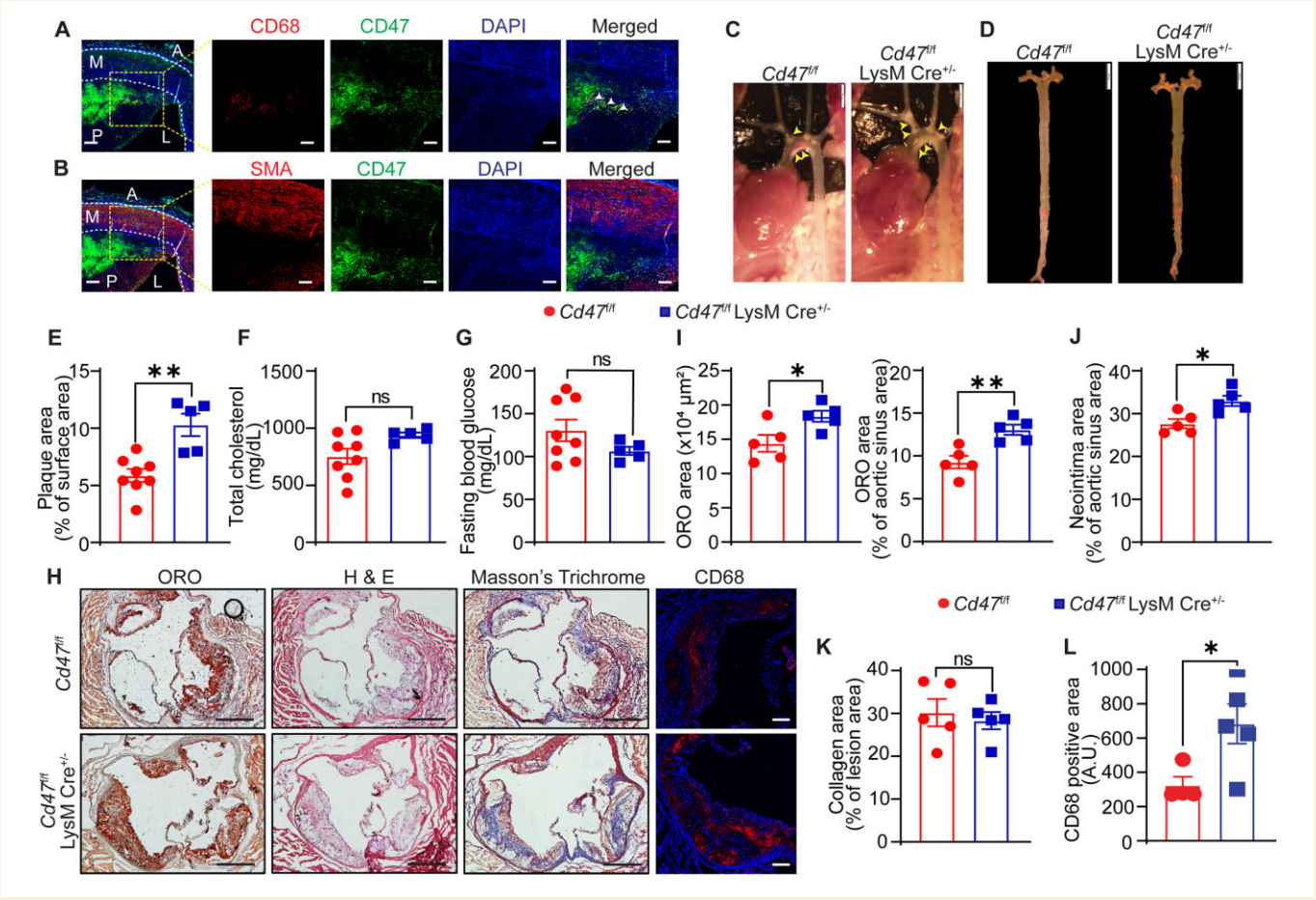


**Figure 4** Myeloid cell-specific CD47 deletion augments atherosclerosis. (*A*) Immunofluorescence staining for CD68 (red), SIRPα (green), and DAPI (blue) was performed on human atherosclerotic LAD cross-sections, scale bar: 50 and 100 µm. Co-localization of CD68 and SIRPα is indicated by white arrowheads ($n = 3$). (*B*) Human LAD cross-sections were immunostained for SMA (red) and SIRPα (green) ($n = 3$), scale bar: 50 and 100 µm. (*C–L*) Male *Cd47*$^{f/f}$ and *Cd47*$^{f/f}$ LysM Cre$^{+/-}$ mice were injected with AAV8-PCSK9 *i.p.*, fed a Western diet for 16 weeks and atherosclerosis analysed. (*C*) Representative *in situ* images of aortic arch (yellow arrowheads point to atherosclerotic lesions), scale bar: 2 mm. (*D*) Representative *en face* ORO staining of aorta, scale bar: 5 mm. (*E*) Quantification of plaque area in aorta ($n = 5–8$). (*F* and *G*) Bar diagrams show total plasma cholesterol (*F*) and fasting blood glucose levels (*G*). (*H*) Representative images of staining performed on aortic root cross-sections, scale bar: 400 µm and CD68, scale bar: 100 µm. (*I–L*) Atherosclerosis area (*I*), neointima area (*J*), collagen content (*K*), and macrophage accumulation (*L*) in aortic root sections ($n = 5$ and CD68 $n = 4–5$). Statistical analyses were performed using a two-tailed unpaired *t*-test. Data represent mean ± SEM. $^*P < 0.05$ and $^{**}P < 0.01$.

blockade of CD47 *in vivo* (i.e. apoptotic cells and phagocyte) needs to be carefully evaluated as direct inhibition of phagocyte CD47 may attenuate phagocytic clearance of apoptotic cells.

## 3.6 Macrophage SIRPα deficiency reduces cholesterol accumulation, improves cholesterol efflux, and suppresses inflammation

Lipid-laden macrophages play a key role in the initiation and progression of atherosclerosis. The role of SIRPα in macrophage function, beyond its ability to regulate efferocytosis, is not well characterized. Next, we investigated whether SIRPα regulates macrophage lipid accumulation, cellular cholesterol metabolism, cholesterol efflux, and inflammation independent of its role in efferocytosis. ORO staining demonstrated significantly decreased lipid accumulation in SIRPα-deficient macrophages following incubation with oxLDL compared with wild-type cells (*Figure 6A and B*). CD36 and SRA1 are high-affinity cell surface receptors for oxLDL and combined deletion of CD36 and SRA1 in macrophages decreases ∼90% of oxLDL uptake.[27] We found that mRNA levels of *Cd36* and *Sra1* were not different between vehicle-treated wild-type and *Sirpa*-knockout macrophages (*Figure 6C and D*). In contrast, *Cd36* levels were significantly up-regulated in oxLDL-treated wild-type, but not in *Sirpa* knockout, macrophages (*Figure 6C*), which may contribute to decreased cholesterol accumulation in SIRPα-deficient macrophages. There were no changes in *Sra1* mRNA levels between control and *Sirpa*-knockout macrophages (*Figure 6D*). Internalization of exogenous LDL is followed by esterification of excess free cholesterol by acyl CoA: cholesterol acyltransferase 1 (ACAT1) and storage of cholesteryl ester (CE) molecules.[28] The hydrolysis of intracellular CE catalyzed by neutral CE hydrolases (NCEH) is a key initial step in cholesterol efflux and reverse cholesterol transport.[28] As shown in *Figure 6E–G*, ACAT1 and NCEH1 expression were

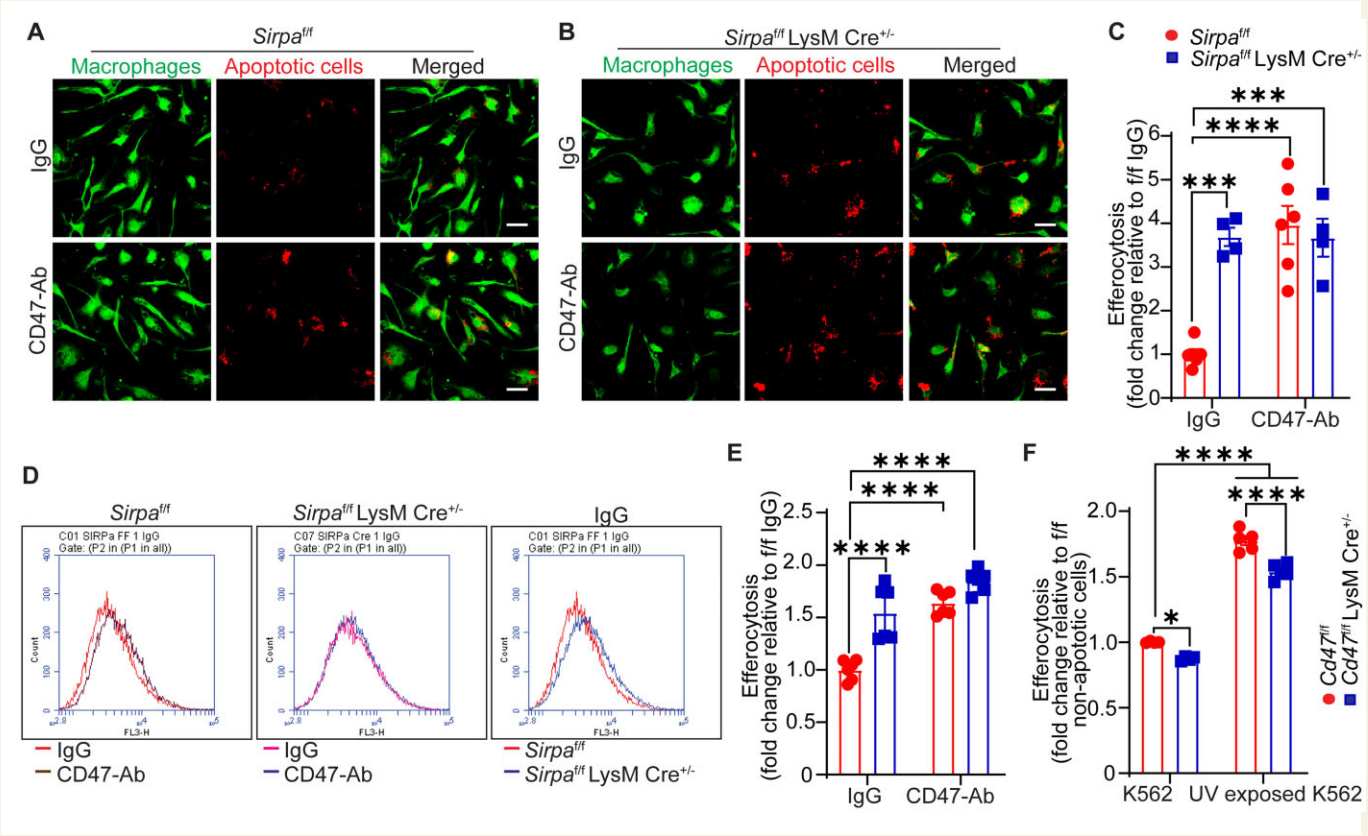


**Figure 5** Macrophage SIRPα deficiency promotes, but macrophage CD47 deletion suppresses efferocytosis. (*A* and *B*) Representative confocal microscopy images showing efferocytosis of apoptotic K562 cells (deep red) by BMM (green) from *Sirpa*$^{f/f}$ (*A*) ($n$ =6) and *Sirpa*$^{f/f}$ LysM Cre$^{+/-}$ mice (*B*) ($n$ =4), scale bar: 20 µm. (*C*) Quantitative data for (*A*) and (*B*). (*D*) Representative flow cytometry histograms demonstrating efferocytosis by BMM from *Sirpa*$^{f/f}$ and *Sirpa*$^{f/f}$ LysM Cre$^{+/-}$ mice ($n$ =6). (*E*) Quantitative data for (*D*). (*F*) Efferocytosis by control and CD47-deficient BMM was determined by flow cytometry ($n$ =4–5). Statistical analyses were performed using a two-way ANOVA followed by Tukey's *post hoc* test. Data represent mean ± SEM. *$P$ < 0.05, ***$P$ < 0.001, and ****$P$ < 0.0001.

not different between wild-type and *Sirpa*-knockout macrophages. Importantly, *Sirpa*-knockout macrophages had enhanced cholesterol efflux compared with wild-type cells (*Figure 6H*), although mRNA levels of ATP-binding cassette subfamily A member 1 (*Abca1*) that mediates plasma membrane efflux of cholesterol were not altered[28] (*Figure 6I*). Taken together, these data suggest that SIRPα deletion protects macrophages from excessive cholesterol accumulation via decreased *Cd36* expression and increased cholesterol efflux.

Macrophage polarization to M1 (pro-inflammatory) or M2 (anti-inflammatory) phenotype is a critical event during the progression or regression of atherosclerosis.[29] To investigate the role of SIRPα in macrophage polarization *in vivo*, aortic root sections from *Sirpa*$^{f/f}$ and *Sirpa*$^{f/f}$ LysM Cre$^{+/-}$ mice were immunostained for CD68 and inducible nitric oxide synthase (iNOS, M1 marker) or arginase 1 (Arg1, M2 marker). Immunostaining analysis displayed elevated Arg1 expression in plaque CD68$^{+}$ cells of *Sirpa*$^{f/f}$ LysM Cre$^{+/-}$ mice compared with *Sirpa*$^{f/f}$ control mice, however, no differences in iNOS expression were observed (*Figure 6J and K*). These data suggest that *Sirpa* deficiency in myeloid cells promotes M2 polarization. Next, we treated BMM from these mice with vehicle or oxLDL, and mRNA levels of various pro-inflammatory cytokines determined. Quantitative PCR data demonstrated reduced *Il6* mRNA levels in SIRPα-depleted macrophages in comparison to wild-type macrophages following oxLDL treatment (*Figure 6L*). The mRNA levels of *Il12, Il1a, Ifnb*, and *Nos2* were not different between control and *Sirpa*-knockout macrophages (*Figure 6M–P*). As shown in Supplementary material online, *Figure S7A–D*, oxLDL treatment increased NFκβ phosphorylation at serine 536 and up-regulated expression of total NFκβ in control macrophages but not in *Sirpa*-knockout cells. Moreover, oxLDL-stimulated NFκβ activation as determined by its nuclear levels was suppressed in SIRPα-deficient macrophages (*Figure 6Q*). Further, plasma levels of anti-inflammatory IL10 were significantly increased in both global and myeloid cell-specific *Sirpa*-knockout mice compared with controls (Supplementary material online, *Figures S8 and S9A*), consistent with the anti-atherosclerotic effects of SIRPα inhibition. Plasma levels of inflammatory cytokines including IL23, IL1, TNFα, MCP1, and IL27 were not different between groups (Supplementary material online, *Figures S8 and S9A*). Taken together, these data indicate that macrophage SIRPα signalling contributes to NFκβ activation *in vitro* and its absence increases anti-inflammatory cytokine levels *in vivo*.

## 3.7 CD47 deletion inhibits macrophage cholesterol efflux and augments inflammation

Next, we investigated cholesterol accumulation, cholesterol efflux, lesional macrophage phenotype, NFκβ activation, and levels of

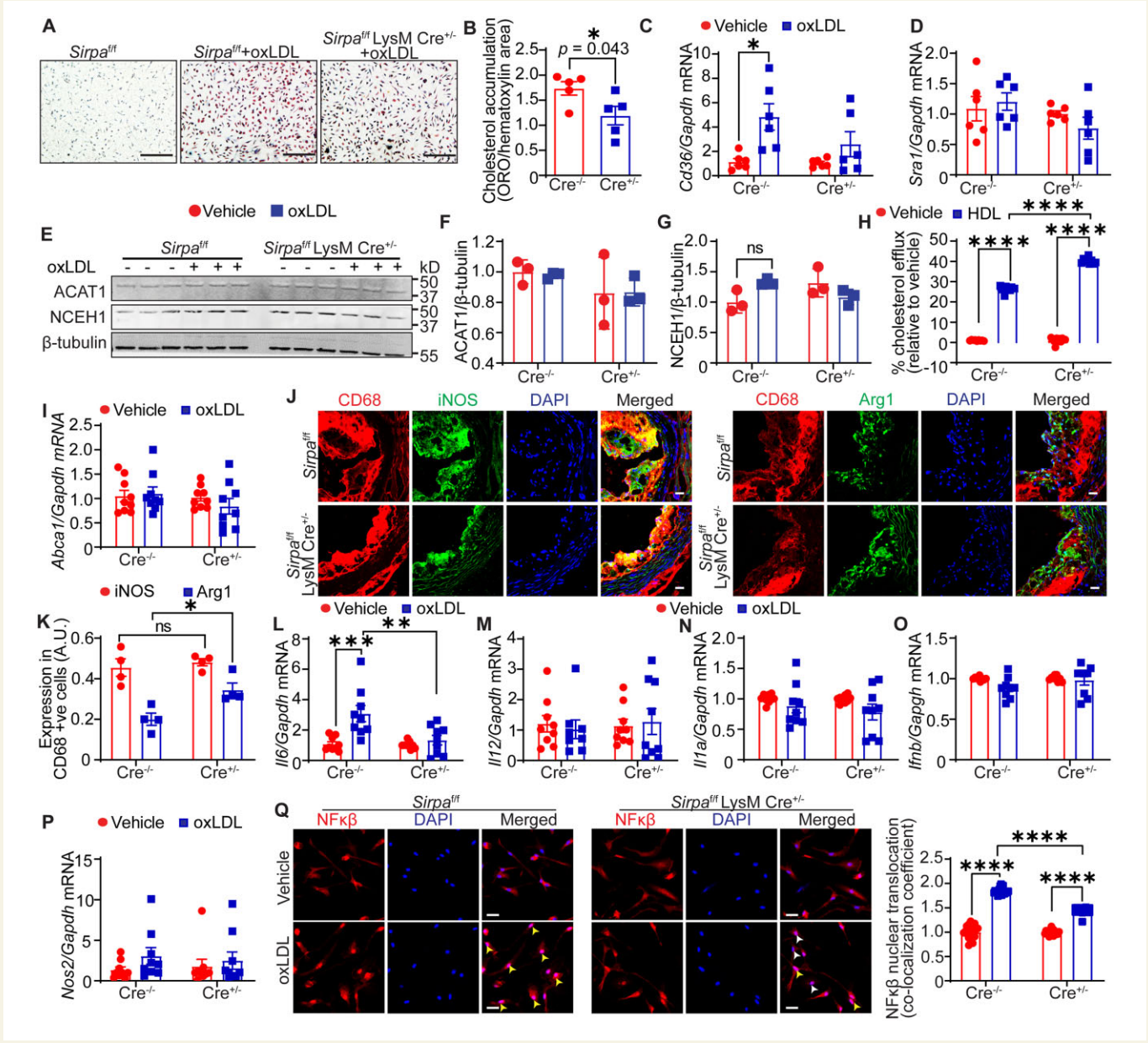


**Figure 6** Macrophage SIRPα deficiency reduces cholesterol accumulation, improves cholesterol efflux and suppresses inflammation. (*A* and *B*) BMM from *Sirpa*$^{f/f}$ and *Sirpa*$^{f/f}$ LysM Cre$^{+/-}$ mice were incubated with oxLDL for 24 h, and cholesterol accumulation investigated. (*A*) Representative images, scale bar: 100 μm. (*B*) Bar diagram shows cholesterol accumulation ($n$ =5). (*C* and *D*) BMM were treated with oxLDL for 24 h and qRT–PCR for *Cd36* and *Sra1* mRNA performed. Bar diagrams show mRNA expression of *Cd36* (*C*) and *Sra1* (*D*). Data are representative of three independent experiments performed in duplicate. (*E–G*) BMM were treated as in (*C* and *D*) and cell lysates utilized for Western blot. (*E*) Representative western blot images. (*F* and *G*) Bar graphs show protein levels normalized to β-tubulin ($n$ = 3). (*H*) Cholesterol efflux by BMM in the absence and presence of HDL. Data are representative of three independent experiments performed in triplicate. (*I* and *L–P*) Macrophages were treated as described above and qRT–PCR performed. Bar diagrams show mRNA levels. Data are representative of three independent experiments performed in triplicate. (*J* and *K*) Aortic root sections from *Sirpa*$^{f/f}$ and *Sirpa*$^{f/f}$ LysM Cre$^{+/-}$ mice were immunostained for CD68, iNOS, and Arg1 ($n$ = 4), scale bar: 20 μm. (*Q*) Representative confocal microscopy images (scale bar: 20 μm) and NFκβ nuclear levels as determined by co-localization of red (NFκβ) and blue (nucleus) colours (yellow arrowheads: nuclei with NFκβ; white arrowheads: nuclei without NFκβ). Data are representative of three independent experiments performed in quintuplicate. Statistical analyses were performed using a two-way ANOVA followed by Tukey's/Bonferroni's *post hoc* test. Data represent mean ± SEM. *$P$ < 0.05, **$P$ < 0.01, ***$P$ < 0.001, and ****$P$ < 0.0001.

inflammatory cytokines in control and CD47 knockout macrophages. No significant changes in cholesterol accumulation were found in CD47-depleted macrophages compared to control cells (*Figure 7A and B*). Treatment with high-density lipoprotein (HDL) enhanced cholesterol efflux by both types of macrophages, however, *Cd47* knockout macrophages had lower cholesterol efflux capacity compared with control

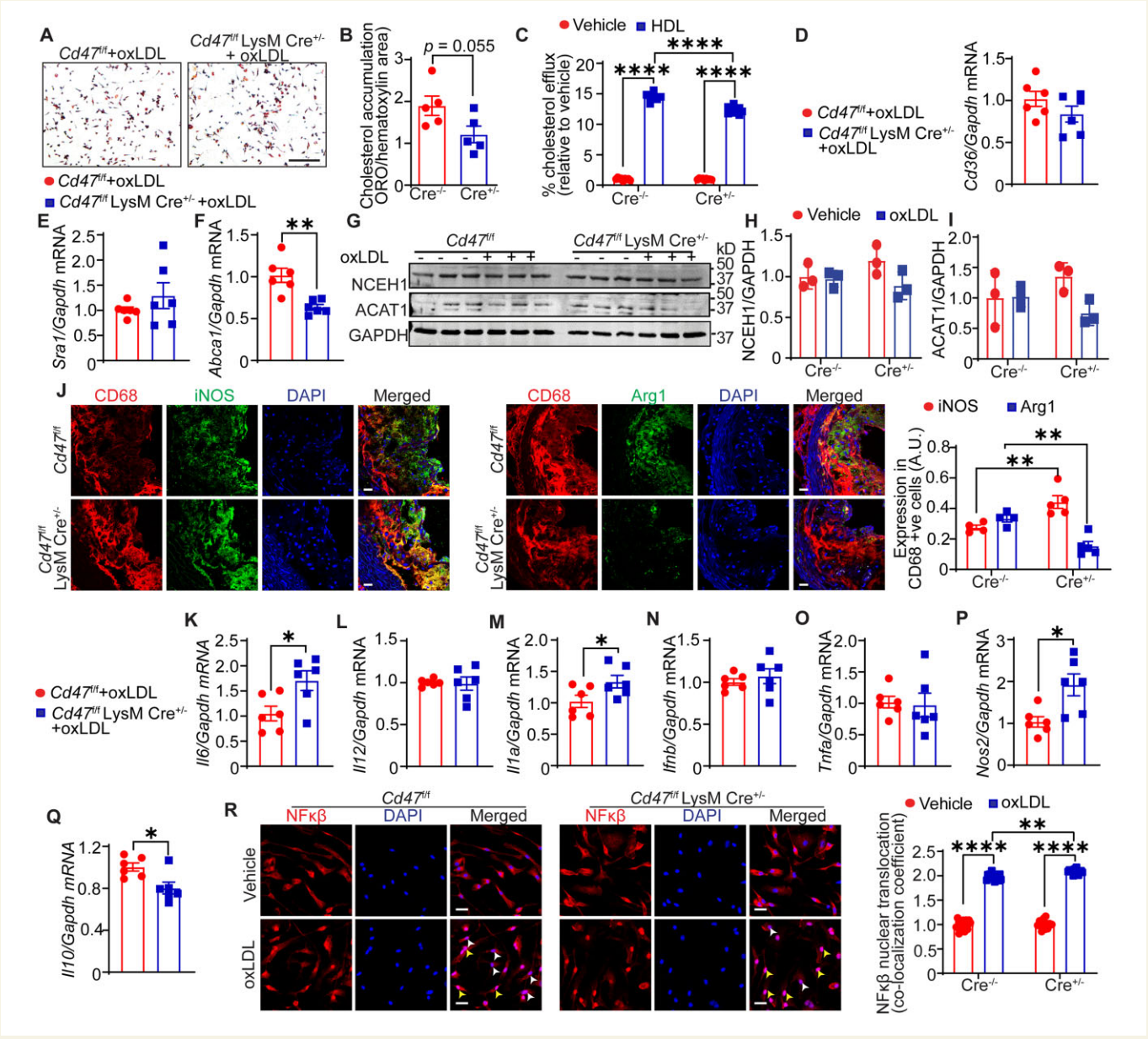


**Figure 7** Macrophage CD47 deletion reduces cholesterol efflux and augments inflammation. (*A* and *B*) BMM were incubated with oxLDL for 24 h and cholesterol accumulation analysed. (*A*) Representative images are shown, scale bar: 100 μm. (*B*) Bar diagram shows cholesterol accumulation ($n$ =5). (*C*) Cholesterol efflux by BMM. Data are representative of three independent experiments performed in triplicate. (*D–N*) Macrophages were treated with oxLDL for 24 h and qRT–PCR/western blot performed. (*D–F*) Bar diagrams show mRNA expression of *Cd36* (*D*), *Sra1* (*E*), and *Abca1* (*F*). Data are representative of three independent experiments performed in duplicate. (*G*) Representative western blot images. (*H* and *I*) Bar graphs show protein expression normalized to GAPDH ($n$ = 3). (*J*) Aortic root sections from *Cd47*$^{f/f}$ and *Cd47*$^{f/f}$ LysM Cre$^{+/-}$ mice were immunostained for CD68, iNOS, and Arg1 ($n$ = 4–5), scale bar: 20 μm. (*K–Q*) Bar diagrams show mRNA levels after oxLDL stimulation. Data are representative of three independent experiments performed in duplicate. (*R*) Representative confocal microscopy images (scale bar: 50 μm) and quantitative data for nuclear NFκβ expression are shown (yellow arrowheads: nuclei with NFκβ; white arrowheads: nuclei without NFκβ). Data are representative of three independent experiments performed in quintuplicate. Statistical analyses were performed using a two-way ANOVA followed by Tukey's *post hoc* test. Data represent mean ± SEM. *$P$ < 0.05, **$P$ < 0.01, ***$P$ < 0.001, and ****$P$ < 0.0001.

macrophages after HDL incubation (*Figure* 7*C*). Further, mRNA levels of *Cd36* and *Sra1* were not different between wild-type and *Cd47* knockout macrophages (*Figure* 7*D and E*). Interestingly, *Cd47* knockout macrophages had reduced *Abca1* mRNA expression in comparison to control cells, which may explain the reduced cholesterol efflux capacity of CD47-depleted macrophages (*Figure* 7*F*). Finally, we observed no differences in NCEH1 and ACAT1 protein levels between different groups (*Figure* 7*G–I*). These findings demonstrate that *Abca1* expression and

cholesterol efflux capacity are decreased in CD47-deficient macrophages compared with control cells.

Immunostaining analysis conducted utilizing aortic root cross-sections of *Cd47*$^{f/f}$ and *Cd47*$^{f/f}$ LysM Cre$^{+/-}$ mice demonstrated decreased Arg1 and increased iNOS expression in lesional CD68$^{+}$ cells of *Cd47*$^{f/f}$ LysM Cre$^{+/-}$ mice in comparison to *Cd47*$^{f/f}$ mice, suggesting augmented M1 polarization in CD47-deficient macrophages (*Figure 7J*). Exposure to oxLDL up-regulated mRNA expression of pro-inflammatory molecules including *Il6, Il1a,* and *Nos2* and reduced levels of anti-inflammatory *Il10* in *Cd47* knockout macrophages compared with wild-type cells (*Figure 7K, M, P and Q*). Oxidized LDL-induced mRNA levels of *Il12, Ifnb,* and *Tnfa* were not different between control and CD47-deficient macrophages (*Figure 7L, N and O*). However, no differences in plasma cytokine levels were observed between *Cd47*$^{f/f}$ and *Cd47*$^{f/f}$ LysM Cre$^{+/-}$ mice (Supplementary material online, *Figure S9B*). Additionally, our confocal experiments demonstrated elevated nuclear NFκβ expression in CD47-depleted macrophages (*Figure 7R*). Similar results were observed when immunoblotting analysis for NFκβ expression performed using nuclear fractions (Supplementary material online, *Figure S7E and F*). Moreover, CD47 loss did not alter serine 536 phosphorylation of NFκβ in macrophages following oxLDL treatment, however, there were increased basal levels of phosphorylated NFκβ in CD47-deficient macrophages (Supplementary material online, *Figure S7G–I*). Taken together, these data indicate that CD47 deletion stimulates NFκβ activation and expression of pro-inflammatory cytokines in macrophages.

### 3.8 Haematological analysis of circulating blood cells in *Cd47* knockout and *Sirpa* mutant mice

CD47 expressed on circulating blood cells serves as a sink for systemically administered CD47 antibodies and leads to haematological side effects including erythrocytopenia, hypohaemoglobinaemia, hyperbilirubinaemia, and thrombocytopenia.[30,31] To investigate haematological changes in *Cd47* knockout and *Sirpa*$^{mut/mut}$ mice, complete blood cell count analysis in wild-type, *Cd47* knockout and *Sirpa*$^{mut/mut}$ mice was performed. The blood analysis demonstrated significantly lower erythrocyte count in *Cd47*-deficient mice (6.8 ± 0.14, $10^6$/μL) compared to wild-type (8.3 ± 0.20, $10^6$/μL) and *Sirpa*$^{mut/mut}$ mice (7.51 ± 0.04, $10^6$/μL) (Supplementary material online, *Figure S10A*). Consistently, haemoglobin levels were significantly lower in *Cd47*-deficient mice (10.38 ± 0.19 g/dL) compared to wild-type (12.18 ± 0.23 g/dL) and *Sirpa*$^{mut/mut}$ mice (11.24 ± 0.17 g/dL) (Supplementary material online, *Figure S10B*). Both erythrocyte count and haemoglobin levels were decreased in *Sirpa*$^{mut/mut}$ mice compared with wild-type controls (Supplementary material online, *Figure S10A and B*). Thrombocyte levels were significantly lower in *Cd47*-deficient mice (467 ± 14.64, $10^3$/μL) compared with wild-type controls (629 ± 47.47, $10^3$/μL) (Supplementary material online, *Figure S10C*). No statistical differences in differential leukocyte levels were found between groups (Supplementary material online, *Figure S10D–G*).

Next, we determined the percentage of myeloid lineage immune cells in the circulation of LysM Cre$^{+/-}$, *Cd47*$^{f/f}$ LysM Cre$^{+/-}$, and *Sirpa*$^{f/f}$ LysM Cre$^{+/-}$ mice using flow cytometry and a haematology autoanalyzer. Both approaches revealed higher percentage of monocytes and neutrophils in *Sirpa*$^{f/f}$ LysM Cre$^{+/-}$ mice compared with control LysM Cre$^{+/-}$ mice (Supplementary material online, *Figure S11A and B*). In addition, *Sirpa*$^{f/f}$ LysM Cre$^{+/-}$ mice had less lymphocytes in circulation compared with *Cd47*$^{f/f}$ LysM Cre$^{+/-}$ and LysM Cre$^{+/-}$ mice (Supplementary material online, *Figure S11A and B*). Further experiments done to investigate CD45$^{+}$ cells in spleen as a measure of total splenic leukocytes suggested reduced percentage of splenic leukocytes in *Sirpa*$^{f/f}$ LysM Cre$^{+/-}$ mice compared with *Cd47*$^{f/f}$ LysM Cre$^{+/-}$ animals (Supplementary material online, *Figure S11C*).

## 4. Discussion

Defective removal of apoptotic cells from atherosclerotic arteries via impaired efferocytosis contributes to arterial inflammation, necrotic core formation, plaque destabilization and rupture, which may lead to adverse cardiovascular events.[8,20] CD47-SIRPα signalling is an important immune checkpoint that inhibits the removal of viable cells with higher CD47 expression to maintain tissue integrity and homeostasis.[30] Apoptotic cells in atherosclerotic lesions have up-regulated CD47 expression, yet, the therapeutic potential of inhibiting the CD47-SIRPα immune checkpoint using pharmacological inhibitors or genetic approaches for the treatment of atherosclerosis remains understudied. Here, using both global and myeloid cell-specific *Sirpa* and *Cd47* knockout mice, human atherosclerotic arteries, and various *in vitro* approaches, we report differential effects of macrophage SIRPα and CD47 deletion on efferocytosis, regulation of cholesterol homeostasis, inflammation, and development of atherosclerosis. Moreover, this is the first study, which has comprehensively analysed the effects of SIRPα vs. CD47 deletion on atherosclerosis development. Our results suggest the advantage of systemic SIRPα blockade over CD47 inhibition to inhibit atherosclerosis development.

Three isoforms of SIRP including SIRPα, SIRPβ, and SIRPγ have been identified.[32] SIRPα binds to CD47 with high affinity and *trans* interaction between CD47 and SIRPα inhibits efferocytosis. SIRPα is a docking protein that recruits and activates SHP-1 and SHP-2 in the plasma membrane to induce depolymerization of cytoskeletal actin and inhibit phagocytosis.[33] To the best of our knowledge, no studies have utilized genetic mouse models to investigate the role of SIRPα in atherosclerosis. To investigate whether SIRPα levels are dysregulated in atherosclerosis, we determined SIRPα expression in both human and murine atherosclerotic and non-atherosclerotic arteries. We found up-regulated SIRPα expression in atherosclerotic IC of aortic arch compared with plaque-free DA segments. Moreover, global *Sirpa*$^{mut/mut}$ mice were protected from atherosclerosis. Consistent with reduced atherosclerosis in hypercholesterolaemic mice treated with a CD47-Ab,[11] we showed that global CD47 deletion prevents atherosclerotic lesion formation. We used two different models of atherosclerosis including AAV8-PCSK9-injected CD47-deficient mice in which LDLR present on hepatocytes is degraded by PCSK9 overexpression[34] and *Apoe*$^{-/-}$/*Cd47*$^{-/-}$ double knockout mice.

Macrophages play a critical role in atherosclerosis.[35] Our immunostaining analysis demonstrates that SIRPα is primarily localized to macrophages in atherosclerotic arteries. Therefore, we next investigated the role of myeloid cell SIRPα in atherosclerosis and showed that myeloid cell-specific SIRPα deletion reduces atherosclerosis development. Defective efferocytosis in atherosclerotic arteries leads to necrotic core formation and enhanced inflammation.[36] In agreement with the role of SIRPα in efferocytosis, we observed smaller necrotic core area in both global *Sirpa* mutant and myeloid cell-specific SIRPα null mice. Flores *et al.*[13] have also shown decreased atherosclerosis in *Apoe*$^{-/-}$ mice-treated with nanoparticles comprising an SHP-1 inhibitor, which abrogates SIRPα-mediated intracellular signalling. Despite the protection from atherosclerosis in global *Cd47* knockout mice, the necrotic core area was not significantly different from wild-type controls. These results

are consistent with a previous study by Engelbertsen *et al.*,[23] although they have found slightly increased atherosclerosis in female CD47-deficient mice. Furthermore, CD47-Ab treatment has been shown to reduce the necrotic area in 4 weeks Western diet-fed-*Apoe*$^{-/-}$ male mice.[11] These differences in atherosclerotic plaque burden and necrotic area among studies by Engelbertsen *et al.*,[23] Kojima *et al.*,[11] and this study could be due to sex differences, methods used to induce atherosclerosis, and duration of Western diet feeding. In addition, female hypercholesterolaemic mice have been shown to develop more atherosclerosis in comparison to male hypercholesterolaemic mice.[37] One should be careful while comparing CD47-Ab treatment with CD47 deletion, as CD47-Ab treatment would block the interaction of its extracellular Ig domain with its extracellular ligands, but not with intracellular proteins, which bind to its cytoplasmic tail. BNIP3 has been recognized as a cytoplasmic binding partner of CD47 and cytoplasmic CD47 tail-BNIP3 interaction regulates autophagy and mitophagy.[38] Further, autophagy has been shown to display both beneficial and detrimental effects in atherosclerosis.[39] Additionally, previous studies identified other binding partners of CD47 cytoplasmic tail.[40] In contrast, CD47 deletion prevents its interaction with both extra- and intracellular ligands. As CD47 is a ubiquitously expressed protein and has multiple binding partners including SIRPα, integrins, VEGFR, and TSP1, antibody blockade of cell surface CD47 and global CD47 deletion are likely to regulate multiple signalling pathways on various cell types in the vessel wall and circulation.[15] For instance, activation of CD47 on endothelial cells by TSP1 has been shown to inhibit angiogenesis via reducing nitric oxide production,[41] and suppression of angiogenesis attenuates atherosclerotic plaque formation.[42] To better address this question, we investigated the role of macrophage CD47 in atherosclerotic lesion formation and observed augmented atherosclerosis in myeloid cell-specific *Cd47* knockout mice. Interestingly, we found comparable necrotic areas in control and myeloid cell-specific CD47-deficient mice. These data suggest a protective role of macrophage CD47 signalling *in vivo* and highlight the importance of cell-specific CD47 inhibition in atherosclerosis. The protective effect of global CD47 inhibition in atherosclerosis may be due to inhibition of SMC CD47 and stimulation of their efferocytic clearance. To date, no previous studies have investigated the role of smooth muscle CD47 in atherosclerosis.

At the cellular level, CD47-Ab treatment enhanced efferocytosis of apoptotic K562 cells by control macrophages; however, SIRPα-deficient macrophages had significantly higher basal efferocytic capacity compared with control macrophages *in vitro*. Consistently, we observed increased efferocytosis in the arterial wall of myeloid cell-specific *Sirpa*-knockout mice. Similarly, inhibition of SHP-1 in macrophages enhanced clearance of apoptotic cells both *in vitro* and *in vivo*.[13] Kojima *et al.*[11] also reported augmented efferocytosis of CD47-Ab-treated apoptotic cells by macrophages. The experimental design, however, in this study was different as apoptotic SMCs were preincubated with CD47-Ab before incubation with phagocytes, which inhibited *trans* SIRPα-CD47 signalling. In our study, inhibition of *cis* signalling in CD47-deficient macrophages attenuated internalization of both control and apoptotic K562 cells, suggesting either direct regulation of phagocytosis by CD47 signalling and/or release of SIRPα from macrophage CD47 interaction. Future studies are required to investigate the underlying mechanisms responsible for impaired efferocytosis in CD47-deficient macrophages. Interestingly, our results are consistent with Bian *et al.*[43] demonstrating reduced red blood cell (RBC) phagocytosis by *Cd47* knockout macrophages. In addition, Lindberg *et al.*[44] demonstrated inhibition of phagocytosis by leukocytes after CD47 deletion. Nonetheless, Wang *et al.*[45] reported increased phagocytosis of latex beads (do not express CD47) by M1-polarized (INF-γ-induced) CD47-deficient macrophages compared with control cells. In these experiments, macrophages were treated with INF-γ to induce M1 polarization. Furthermore, Wang *et al.* showed differences in phagocytic capacity of M0 and M1 macrophages. These contradictory observations might be due to utilizing differently polarized macrophages for phagocytosis experiments in this study and by Wang *et al.*[45] Further efferocytosis is an actin-dependent process, earlier studies have suggested the role of CD47 in regulating actin remodelling.[46] In addition, SIRPα-CD47 interaction is not the only signalling axis regulating efferocytosis. Lower expression of 'eat-me' signal calreticulin, reduced expression and function of efferocytic receptors and their bridging molecules, competition between apoptotic cells and lipids to bind efferocytic receptors, and inflammation-induced reduction in levels of various key efferocytosis molecules may all be involved in reduced efferocytosis in atherosclerotic arteries.[8] It is also possible that macrophage SIRPα or CD47 deficiency may have indirect effects on key efferocytosis molecules and interactions.

As oxLDL is a well-known pro-atherogenic and pro-inflammatory molecule, we utilized oxLDL to determine the role of macrophage SIRPα and CD47 in cholesterol accumulation and inflammation independent of efferocytosis.[47] SIRPα-deficient macrophages displayed reduced cholesterol accumulation, increased cholesterol efflux, and attenuated *Il6* levels after oxLDL exposure. In addition, oxLDL treatment up-regulated *Cd36* mRNA expression in control macrophages, but not in SIRPα-deleted macrophages, which may be responsible for reduced cholesterol accumulation in *Sirpa*-knockout macrophages. Consistently, previous studies have shown up-regulation of CD36 levels following oxLDL treatment via PKC- and PPARγ-dependent mechanisms.[48,49] No differences in the expression of key molecules involved in cholesterol handling and transport (ACAT, NCEH1, and *Abca1*) were observed in *Sirpa*-knockout macrophages. Arg1 (M2 macrophage marker) expression was elevated in CD68$^{+}$ areas of atherosclerotic arteries isolated from myeloid cell-specific *Sirpa*-knockout mice, which is consistent with improved *in vivo* efferocytosis in these mice.[50] Increased plasma levels of IL10 in global *Sirpa* mutant and myeloid cell-specific *Sirpa*-knockout mice suggest reduced systemic inflammation. In addition, SIRPα-deficient macrophages showed reduced nuclear translocation of NFκβ following oxLDL stimulation, which may provide a mechanistic link between SIRPα and regulation of inflammatory processes as NFκβ signalling is known to stimulate pro-inflammatory molecules, such as IL6.[51] On the contrary, macrophage CD47 deletion reduced cholesterol efflux, induced levels of pro-inflammatory molecules *in vivo* and *in vitro*, and enhanced nuclear NFκβ expression, which coincide with increased atherosclerosis in myeloid cell-specific *Cd47* knockout mice. Additional experiments demonstrating decreased activation of NFκβ in *Sirpa*-knockout macrophages following oxLDL stimulation, and increased basal levels of phosphorylated NFκβ in CD47-deleted macrophages, suggest pro-inflammatory and anti-inflammatory roles of macrophage SIRPα and CD47, respectively.

CD47- and SIRPα-blocking antibodies are in clinical trials.[5,6] Moreover, CD47-Ab treatment has been shown to reduce vascular inflammation in patients with relapsed/refractory B-cell non-Hodgkin's lymphoma.[12] The use of CD47-Ab may have effects independent of efferocytosis. In addition, CD47-Ab treatment leads to side effects including erythrocytopenia, hypohaemoglobinaemia, and thrombocytopenia.[11,30,31,52] Consistent with this, our haematological analysis showed reduced RBC count and haemoglobin levels in *Cd47* knockout mice compared with wild-type and *Sirpa*$^{mut/mut}$ mice. Circulating platelet levels

were also significantly lower in *Cd47*-deficient mice in comparison to wild-type controls. SIRPα expression is limited to certain cell types including neurons and myeloid cells, nonetheless, inhibition of SIRPα-mediated signalling may have neurological side effects. Selective blockade of SIRPα-mediated signalling may be a more viable strategy to circumvent haematological side effects observed using CD47-Ab and may serve as an effective therapeutic strategy for patients with CVD. In our study, majority of mouse lines except $Cd47^{-/-}$ mice (12 weeks) were fed a Western diet for 16 weeks. These differences in dietary period may prevent the direct comparison of atherosclerosis among $Cd47^{-/-}$ mice and other mouse lines. The findings of the present study warrant future investigations evaluating (i) the mechanisms regulating SIRPα expression in atherosclerotic arteries, (ii) investigating whether TSP1 attenuates SIRPα-CD47 interaction and regulates lesional efferocytosis, (iii) role of SIRPα expressed on T cells and dendritic cells in atherosclerosis, and (iv) as integrin activation has been shown to stimulate phagocytosis of cancer cells by macrophages,[53] it would be interesting to investigate the combined effects of integrin activation and SIRPα-blocking antibody treatment in the context of atherosclerosis development.

In conclusion, to our knowledge, these findings provide the first evidence that global *Sirpa* mutant and myeloid cell-specific SIRPα-deficient mice are protected from atherosclerosis, while deletion of CD47 selectively in myeloid cells augments atherosclerotic lesion formation. These results identify SIRPα as a potential therapeutic target in atherosclerosis.

# Supplementary material

Supplementary material is available at *Cardiovascular Research* online.

# Authors' contributions

B.S. and G.C. designed the study. B.S. performed most of the experiments, analysed data, and wrote the manuscript. H.-P.L. helped with experiments. W.A. and M.S. performed image analysis. J.X., Q.M., and Y.H. assisted with mouse whole blood analysis. K.D. and J.Z. helped with gene expression data analysis (GSE43292) of human atherosclerotic and non-atherosclerotic carotid endarterectomy samples. M.C.-S. recorded weight of mice weekly. J.W. provided non-atherosclerotic and atherosclerotic human arterial tissue. G.C. provided feedback on experiments, reviewed and edited the manuscript.

## Acknowledgements

We are thankful to Drs Yuqing Huo, David Stepp, and Muhammad Ashraf, Augusta University, for allowing us to use their phase-contrast microscope & stereomicroscope, NMR machine, and cryostat, respectively. We are also grateful to David Adams and David Johnson, Department of Cellular Biology & Anatomy, Augusta University for providing us human cadaveric tissue for research purposes.

**Conflict of interest:** The authors declare no conflict of interest.

## Funding

This work was supported by the National Institutes of Health grants [R01HL139562 and R00HL114648 awarded to G.C., and K99HL146954 and R00146954 given to B.S.] and American Heart Association Postdoctoral Fellowship [17POST33661254 given to B.S.].

## Data availability

The data relating to this article are available in the article itself or in its Supplementary material online.

## References

1. Pardoll DM. The blockade of immune checkpoints in cancer immunotherapy. *Nat Rev Cancer* 2012;**12**:252–264.
2. Chao MP, Majeti R, Weissman IL. Programmed cell removal: a new obstacle in the road to developing cancer. *Nat Rev Cancer* 2011;**12**:58–67.
3. Chao MP, Tang C, Pachynski RK, Chin R, Majeti R, Weissman IL. Extranodal dissemination of non-Hodgkin lymphoma requires CD47 and is inhibited by anti-CD47 antibody therapy. *Blood* 2011;**118**:4890–4901.
4. Tseng D, Volkmer JP, Willingham SB, Contreras-Trujillo H, Fathman JW, Fernhoff NB, Seita J, Inlay MA, Weiskopf K, Miyanishi M, Weissman IL. Anti-CD47 antibody-mediated phagocytosis of cancer by macrophages primes an effective antitumor T-cell response. *Proc Natl Acad Sci USA* 2013;**110**:11103–11108.
5. Andrejeva G, Capoccia BJ, Hiebsch RR, Donio MJ, Darwech IM, Puro RJ, Pereira DS. Novel SIRPalpha antibodies that induce single-agent phagocytosis of tumor cells while preserving T cells. *J Immunol* 2021;**206**:712–721.
6. Jeanne A, Schneider C, Martiny L, Dedieu S. Original insights on thrombospondin-1-related antireceptor strategies in cancer. *Front Pharmacol* 2015;**6**:252.
7. Karmali KN, Lloyd-Jones DM, Berendsen MA, Goff DC Jr, Sanghavi DM, Brown NC, Korenovska L, Huffman MD. Drugs for primary prevention of atherosclerotic cardiovascular disease: an overview of systematic reviews. *JAMA Cardiol* 2016;**1**:341–349.
8. Yurdagul A Jr, Doran AC, Cai B, Fredman G, Tabas IA. Mechanisms and consequences of defective efferocytosis in atherosclerosis. *Front Cardiovasc Med* 2017;**4**:86.
9. Libby P. The changing landscape of atherosclerosis. *Nature* 2021;**592**:524–533.
10. Schrijvers DM, De Meyer GR, Kockx MM, Herman AG, Martinet W. Phagocytosis of apoptotic cells by macrophages is impaired in atherosclerosis. *Arterioscler Thromb Vasc Biol* 2005;**25**:1256–1261.
11. Kojima Y, Volkmer JP, McKenna K, Civelek M, Lusis AJ, Miller CL, Direnzo D, Nanda V, Ye J, Connolly AJ, Schadt EE, Quertermous T, Betancur P, Maegdefessel L, Matic LP, Hedin U, Weissman IL, Leeper NJ. CD47-blocking antibodies restore phagocytosis and prevent atherosclerosis. *Nature* 2016;**536**:86–90.
12. Jarr KU, Nakamoto R, Doan BH, Kojima Y, Weissman IL, Advani RH, Iagaru A, Leeper NJ. Effect of CD47 blockade on vascular inflammation. *N Engl J Med* 2021;**384**:382–383.
13. Flores AM, Hosseini-Nassab N, Jarr KU, Ye J, Zhu X, Wirka R, Koh AL, Tsantilas P, Wang Y, Nanda V, Kojima Y, Zeng Y, Lotfi M, Sinclair R, Weissman IL, Ingelsson E, Smith BR, Leeper NJ. Pro-efferocytic nanoparticles are specifically taken up by lesional macrophages and prevent atherosclerosis. *Nat Nanotechnol* 2020;**15**:154–161.
14. Oronsky B, Carter C, Reid T, Brinkhaus F, Knox SJ. Just eat it: a review of CD47 and SIRP-alpha antagonism. *Semin Oncol* 2020;**47**:117–124.
15. Sick E, Jeanne A, Schneider C, Dedieu S, Takeda K, Martiny L. CD47 update: a multifaceted actor in the tumour microenvironment of potential therapeutic interest. *Br J Pharmacol* 2012;**167**:1415–1430.
16. Barclay AN, Van den Berg TK. The interaction between signal regulatory protein alpha (SIRPalpha) and CD47: structure, function, and therapeutic target. *Annu Rev Immunol* 2014;**32**:25–50.
17. Adams S, van der Laan LJ, Vernon-Wilson E, Renardel de Lavalette C, Döpp EA, Dijkstra CD, Simmons DL, van den Berg TK. Signal-regulatory protein is selectively expressed by myeloid and neuronal cells. *J Immunol* 1998;**161**:1853–1859.
18. Singla B, Lin HP, Chen A, Ahn W, Ghoshal P, Cherian-Shaw M, White J, Stansfield BK, Csanyi G. Role of R-spondin 2 in arterial lymphangiogenesis and atherosclerosis. *Cardiovasc Res* 2020;**117**:1489–1509.
19. Ayari H, Bricca G. Identification of two genes potentially associated in iron-heme homeostasis in human carotid plaque using microarray analysis. *J Biosci* 2013;**38**:311–315.
20. Hansson GK, Libby P, Tabas I. Inflammation and plaque vulnerability. *J Intern Med* 2015;**278**:483–493.
21. Inagaki K, Yamao T, Noguchi T, Matozaki T, Fukunaga K, Takada T, Hosooka T, Akira S, Kasuga M. SHPS-1 regulates integrin-mediated cytoskeletal reorganization and cell motility. *EMBO J* 2000;**19**:6721–6731.
22. Wu J, Dong J, Verzola D, Hruska K, Garibotto G, Hu Z, Mitch WE, Thomas SS. Signal regulatory protein alpha initiates cachexia through muscle to adipose tissue crosstalk. *J Cachexia Sarcopenia Muscle* 2019;**10**:1210–1227.
23. Engelbertsen D, Autio A, Verwilligen RAF, Depuydt MAC, Newton G, Rattik S, Levinsohn E, Saggu G, Jarolim P, Wang H, Velazquez F, Lichtman AH, Luscinskas FW. Increased lymphocyte activation and atherosclerosis in CD47-deficient mice. *Sci Rep* 2019;**9**:10608.
24. Tan S, Zhao J, Sun Z, Cao S, Niu K, Zhong Y, Wang H, Shi L, Pan H, Hu J, Qian L, Liu N, Yuan J. Hepatocyte-specific TAK1 deficiency drives RIPK1 kinase-dependent inflammation to promote liver fibrosis and hepatocellular carcinoma. *Proc Natl Acad Sci USA* 2020;**117**:14231–14242.

25. Stary HC, Chandler AB, Dinsmore RE, Fuster V, Glagov S, Insull W Jr, Rosenfeld ME, Schwartz CJ, Wagner WD, Wissler RW. A definition of advanced types of atherosclerotic lesions and a histological classification of atherosclerosis. A report from the Committee on Vascular Lesions of the Council on Arteriosclerosis, American Heart Association. *Circulation* 1995;**92**:1355–1374.
26. Dheilly E, Moine V, Broyer L, Salgado-Pires S, Johnson Z, Papaioannou A, Cons L, Calloud S, Majocchi S, Nelson R, Rousseau F, Ferlin W, Kosco-Vilbois M, Fischer N, Masternak K. Selective blockade of the ubiquitous checkpoint receptor CD47 is enabled by dual-targeting bispecific antibodies. *Mol Ther* 2017;**25**:523–533.
27. Kunjathoor VV, Febbraio M, Podrez EA, Moore KJ, Andersson L, Koehn S, Rhee JS, Silverstein R, Hoff HF, Freeman MW. Scavenger receptors class A-I/II and CD36 are the principal receptors responsible for the uptake of modified low density lipoprotein leading to lipid loading in macrophages. *J Biol Chem* 2002;**277**:49982–49988.
28. Sekiya M, Osuga J, Nagashima S, Ohshiro T, Igarashi M, Okazaki H, Takahashi M, Tazoe F, Wada T, Ohta K, Takanashi M, Kumagai M, Nishi M, Takase S, Yahagi N, Yagyu H, Ohashi K, Nagai R, Kadowaki T, Furukawa Y, Ishibashi S. Ablation of neutral cholesterol ester hydrolase 1 accelerates atherosclerosis. *Cell Metab* 2009;**10**:219–228.
29. Peled M, Fisher EA. Dynamic aspects of macrophage polarization during atherosclerosis progression and regression. *Front Immunol* 2014;**5**:579.
30. Oldenborg PA, Zheleznyak A, Fang YF, Lagenaur CF, Gresham HD, Lindberg FP. Role of CD47 as a marker of self on red blood cells. *Science* 2000;**288**:2051–2054.
31. Olsson M, Bruhns P, Frazier WA, Ravetch JV, Oldenborg PA. Platelet homeostasis is regulated by platelet expression of CD47 under normal conditions and in passive immune thrombocytopenia. *Blood* 2005;**105**:3577–3582.
32. Barclay AN, Brown MH. The SIRP family of receptors and immune regulation. *Nat Rev Immunol* 2006;**6**:457–464.
33. Matozaki T, Murata Y, Okazawa H, Ohnishi H. Functions and molecular mechanisms of the CD47-SIRPalpha signalling pathway. *Trends Cell Biol* 2009;**19**:72–80.
34. Lu H, Howatt DA, Balakrishnan A, Graham MJ, Mullick AE, Daugherty A. Hypercholesterolemia induced by a PCSK9 gain-of-function mutation augments angiotensin II-induced abdominal aortic aneurysms in C57BL/6 mice-brief report. *Arterioscler Thromb Vasc Biol* 2016;**36**:1753–1757.
35. Moore KJ, Sheedy FJ, Fisher EA. Macrophages in atherosclerosis: a dynamic balance. *Nat Rev Immunol* 2013;**13**:709–721.
36. Moore KJ, Tabas I. Macrophages in the pathogenesis of atherosclerosis. *Cell* 2011;**145**:341–355.
37. Smith DD, Tan X, Tawfik O, Milne G, Stechschulte DJ, Dileepan KN. Increased aortic atherosclerotic plaque development in female apolipoprotein E-null mice is associated with elevated thromboxane A2 and decreased prostacyclin production. *J Physiol Pharmacol* 2010;**61**:309–316.
38. Soto-Pantoja DR, Kaur S, Roberts DD. CD47 signaling pathways controlling cellular differentiation and responses to stress. *Crit Rev Biochem Mol Biol* 2015;**50**:212–230.
39. Martinet W, De Meyer GR. Autophagy in atherosclerosis: a cell survival and death phenomenon with therapeutic potential. *Circ Res* 2009;**104**:304–317.
40. Wu AL, Wang J, Zheleznyak A, Brown EJ. Ubiquitin-related proteins regulate interaction of vimentin intermediate filaments with the plasma membrane. *Mol Cell* 1999;**4**:619–625.
41. Bauer EM, Qin Y, Miller TW, Bandle RW, Csanyi G, Pagano PJ, Bauer PM, Schnermann J, Roberts DD, Isenberg JS. Thrombospondin-1 supports blood pressure by limiting eNOS activation and endothelial-dependent vasorelaxation. *Cardiovasc Res* 2010;**88**:471–481.
42. Moulton KS, Heller E, Konerding MA, Flynn E, Palinski W, Folkman J. Angiogenesis inhibitors endostatin or TNP-470 reduce intimal neovascularization and plaque growth in apolipoprotein E-deficient mice. *Circulation* 1999;**99**:1726–1732.
43. Bian Z, Shi L, Guo YL, Lv Z, Tang C, Niu S, Tremblay A, Venkataramani M, Culpepper C, Li L, Zhou Z, Mansour A, Zhang Y, Gewirtz A, Kidder K, Zen K, Liu Y. Cd47-Sirpalpha interaction and IL-10 constrain inflammation-induced macrophage phagocytosis of healthy self-cells. *Proc Natl Acad Sci USA* 2016;**113**:E5434–E5443.
44. Lindberg FP, Bullard DC, Caver TE, Gresham HD, Beaudet AL, Brown EJ. Decreased resistance to bacterial infection and granulocyte defects in IAP-deficient mice. *Science* 1996;**274**:795–798.
45. Wang Y, Nanda V, Direnzo D, Ye J, Xiao S, Kojima Y, Howe KL, Jarr KU, Flores AM, Tsantilas P, Tsao N, Rao A, Newman AAC, Eberhard AV, Priest JR, Ruusalepp A, Pasterkamp G, Maegdefessel L, Miller CL, Lind L, Koplev S, Bjorkegren JLM, Owens GK, Ingelsson E, Weissman IL, Leeper NJ. Clonally expanding smooth muscle cells promote atherosclerosis by escaping efferocytosis and activating the complement cascade. *Proc Natl Acad Sci USA* 2020;**117**:15818–15826.
46. Yoshida H, Tomiyama Y, Ishikawa J, Oritani K, Matsumura I, Shiraga M, Yokota T, Okajima Y, Ogawa M, Miyagawa J, Nishiura T, Matsuzawa Y. Integrin-associated protein/CD47 regulates motile activity in human B-cell lines through CDC42. *Blood* 2000;**96**:234–241.
47. Lara-Guzmán OJ, Gil-Izquierdo Á, Medina S, Osorio E, Álvarez-Quintero R, Zuluaga N, Oger C, Galano J-M, Durand T, Muñoz-Durango K. Oxidized LDL triggers changes in oxidative stress and inflammatory biomarkers in human macrophages. *Redox Biol* 2018;**15**:1–11.
48. Feng J, Han J, Pearce SF, Silverstein RL, Gotto AM Jr, Hajjar DP, Nicholson AC. Induction of CD36 expression by oxidized LDL and IL-4 by a common signaling pathway dependent on protein kinase C and PPAR-gamma. *J Lipid Res* 2000;**41**:688–696.
49. Nagy L, Tontonoz P, Alvarez JG, Chen H, Evans RM. Oxidized LDL regulates macrophage gene expression through ligand activation of PPARgamma. *Cell* 1998;**93**:229–240.
50. Yurdagul A Jr, Subramanian M, Wang X, Crown SB, Ilkayeva OR, Darville L, Kolluru GK, Rymond CC, Gerlach BD, Zheng Z, Kuriakose G, Kevil CG, Koomen JM, Cleveland JL, Muoio DM, Tabas I. Macrophage metabolism of apoptotic cell-derived arginine promotes continual efferocytosis and resolution of injury. *Cell Metab* 2020;**31**:518–533.e510.
51. Brasier AR. The nuclear factor-kappaB-interleukin-6 signalling pathway mediating vascular inflammation. *Cardiovasc Res* 2010;**86**:211–218.
52. Sikic BI, Lakhani N, Patnaik A, Shah SA, Chandana SR, Rasco D, Colevas AD, O'Rourke T, Narayanan S, Papadopoulos K, Fisher GA, Villalobos V, Prohaska SS, Howard M, Beeram M, Chao MP, Agoram B, Chen JY, Huang J, Axt M, Liu J, Volkmer JP, Majeti R, Weissman IL, Takimoto CH, Supan D, Wakelee HA, Aoki R, Pegram MD, Padda SK. First-in-human, first-in-class phase I trial of the anti-CD47 antibody Hu5F9-G4 in patients with advanced cancers. *J Clin Oncol* 2019;**37**:946–953.
53. Morrissey MA, Kern N, Vale RD. CD47 ligation repositions the inhibitory receptor SIRPA to suppress integrin activation and phagocytosis. *Immunity* 2020;**53**:290–302.e296.


## Translational perspective

Despite the extensive use of lipid-lowering and anti-hypertensive drugs, atherosclerotic plaque rupture responsible for myocardial infarction and stroke remains the leading cause of death worldwide. Although stimulation of phagocytic removal of apoptotic cells in atherosclerotic arteries to preserve lesion stability seems an attractive therapeutic strategy, comprehensive genetic studies using preclinical models are still lacking. Using human atherosclerotic arteries, global and myeloid cell-specific CD47 and SIRPα knockout mice and *in vitro* techniques, we identify SIRPα as a potential therapeutic target in atherosclerosis. Further, our results suggest that cell-specific inhibition of CD47 could also be considered as a future therapeutic strategy.